

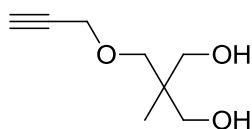
Supporting Information to

Synthesis of Alkyne Functional Cyclic Polymers by One-pot Thiol-ene Cyclization.

Derong Lu, Zhongfan Jia and Michael J. Monteiro**

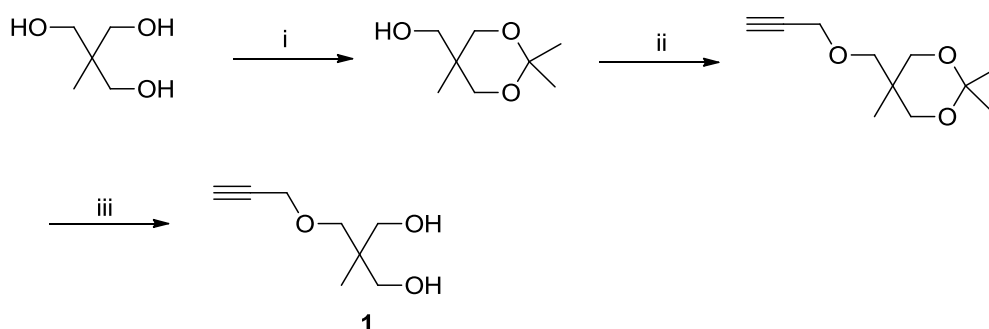
1. Australian Institute for Bioengineering and Nanotechnology, University of Queensland, Brisbane QLD 4072, Australia

1 Synthesis of 2-methyl-2-((prop-2-yn-1-yloxy)methyl)propane-1,3-diol



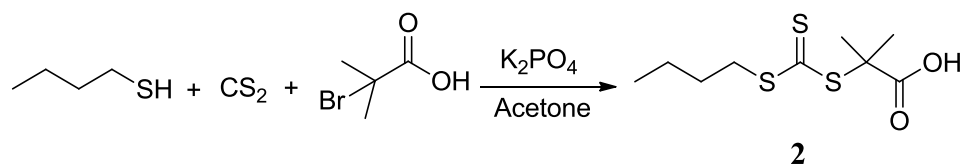
This compound was synthesized according to literature procedure¹.

Scheme S1: The reaction route of the synthesis of 2-methyl-2- ((prop-2-yn-1-yloxy) methyl) propane-1,3-diol



i) Acetone, p-TsOH, RT, 16 h; ii) THF, NaH, propargyl bromide, -78 °C to R.T., 16 h; iii) DOWEX, Methanol, R.T. 16 h;

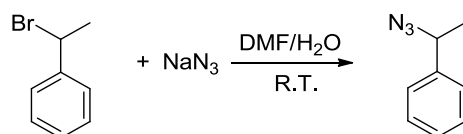
2 Synthesis of the 2-(((butylthio)carbonothioyl)thio)-2-methylpropanoic acid(2)



The 2-(((butylthio)carbonothioyl)thio)-2-methylpropanoic acid was synthesized according to the literature procedure². A mixture of 11.76 g (5.540×10^{-2} mol) K_3PO_4 and 100 mL acetone was allowed to stir for 6 h, 5.938 mL (5.540×10^{-2} mol) 1-butanethiol and 10 mL (5.540×10^{-2} mol) carbondisulfide were added into the solution above and kept stirring for 1h. After that 8.35 g (5.0×10^{-2} mol) bromoisobutyric acid was added dropwise to a stirring solution above over a period of 30 min at 0 °C under an argon atmosphere. The reaction was stirring overnight and warmed up to R.T. The reaction mixture was filtered to remove the solid, concentrated and applied under vacuum at R.T. The solution was then washed with cold 10% HCl solution (3 x 50 mL) and distilled water (2 x 50 mL) and dried over anhydrous $MgSO_4$. The solvent was removed under vacuum, and the residual crude product was purified by column chromatography with EtOAc / petroleum spirit (3/2, v/v) as eluent. The fraction with R_f as 0.45 was collected, concentrated, recrystallized into n-Hexane, dried under the vacuum at R.T., and orange solid product **2** was obtained with the yield as 68.5 %.

1H NMR ($CDCl_3$, 298 K, 300 MHz): δ 3.27 (t, 2H; $J=7.38$ Hz; $-CH_2-CH_2-S-$), 1.70 (s, 6H; $(CH_3)_2-C-$), 1.64 (m, 2H, $J=8.94$ Hz; $-CH_2-CH_2-CH_2-$), 1.41 (m, 2H; $J=7.29$ Hz; $CH_3-CH_2-CH_2-$), 0.90 (t, 3H, $J=7.26$ Hz; $CH_3-CH_2-CH_2-$); ^{13}C NMR ($CDCl_3$, 298 K, 300 MHz): 228.3, 128.9, 55.6, 36.7, 29.8, 25.2, 22.1, 13.6.

3 Synthesis of (1-azidoethyl) benzene



(1-bromomethyl)-benzene (3.0 g, 16.2 mmol) and sodium azide (2.1 g, 32.4 mmol) were dissolved in a mixture of DMF (9 mL) and water (1 mL) and the resulting solution was stirred overnight. The mixture was added 30 mL brine and extracted with diethyl ether (3 x 60 mL). The organic layer collected were dried over anhydrous MgSO_4 , after removal of the solvent under reduced pressure, colourless oil (1-azidoethyl) benzene was obtained with yield as 84 %.

^1H NMR (CDCl_3 , 298 K, 400 MHz): δ 7.45 (d, 2H, $J=7.48$, benzene protons), 7.35 (dd, 2H, $J=8.28$ Hz, 7.40 Hz; benzene protons), 7.29 (d, 1H, $J=7.12$ Hz; benzene proton), 4.60 (q, 1H, $J=6.92$ Hz; $\text{CH}_3\text{-CH-N}_3$), 1.53 (d, 3H; $J=6.92$ Hz; methyl protons); ^{13}C NMR (CDCl_3 , 298 K, 400 MHz); 140.9, 128.7, 128.1, 126.3, 61.1, 21.6.

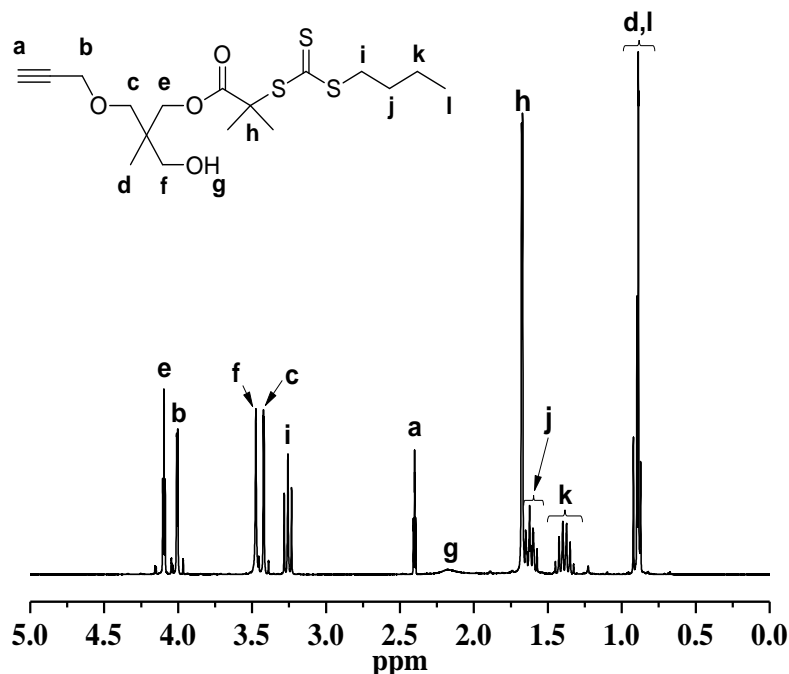


Figure S1: ^1H NMR spectrum (300 MHz) of α -hydroxyl- α' -alkyne RAFT agent **3** in CDCl_3 at 298 K.

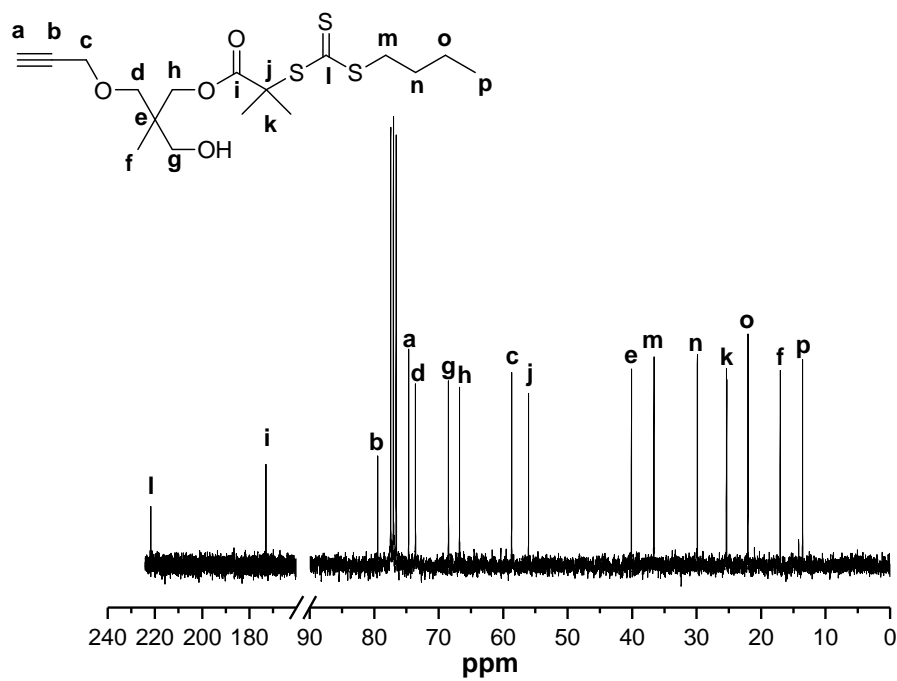


Figure S2: ¹³C NMR spectrum (300 MHz) of **3** in CDCl₃ at 298 K.

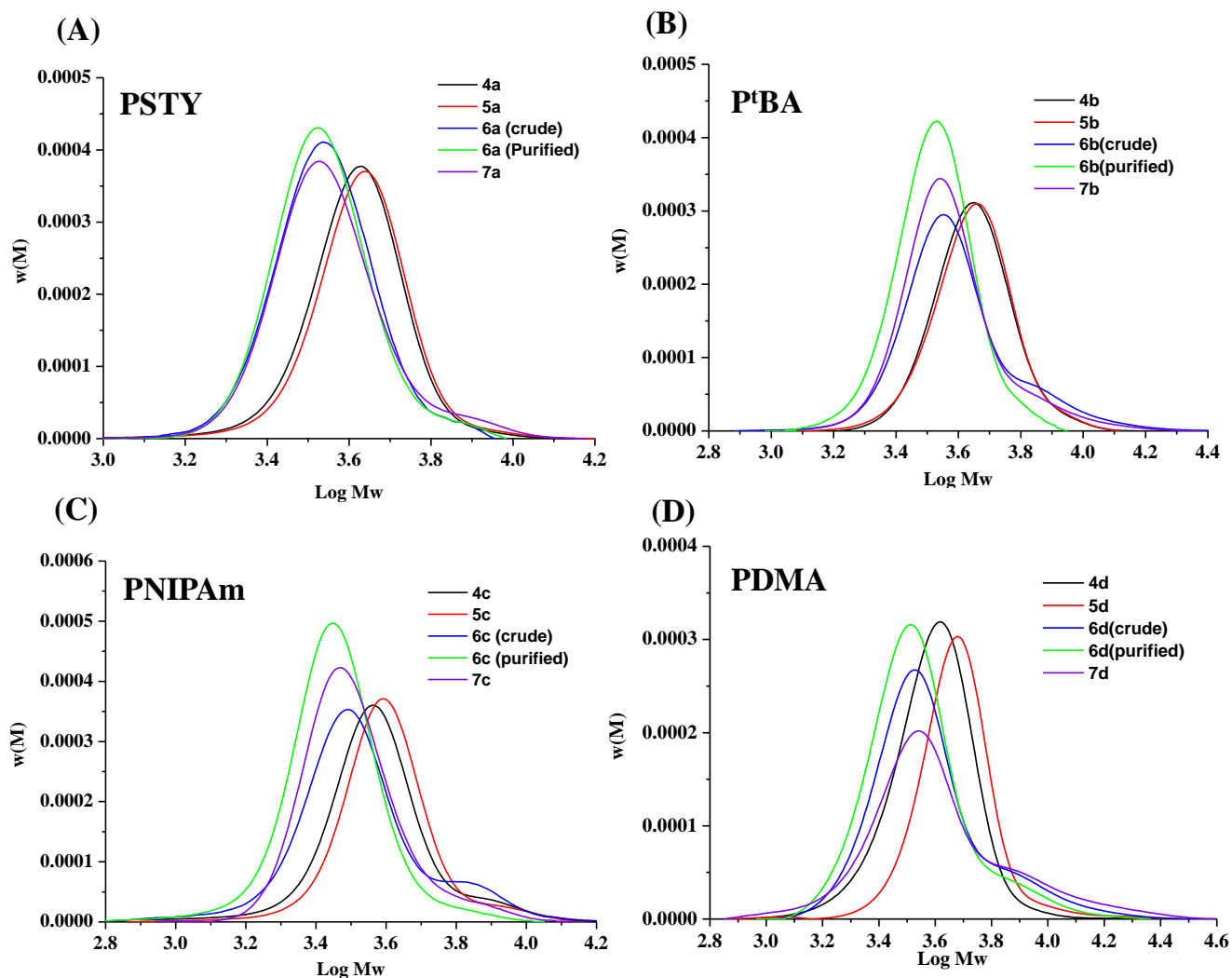


Figure S3: Overall SEC traces of polymers **4**, **5**, **6**, and **7**. (A) for **a**, (B) for **b**, and (C) for **c** were determined from THF SEC, RI detector, PSTY standard; (D) for **d** was determined from DMAc SEC, RI detector, PSTY standard.

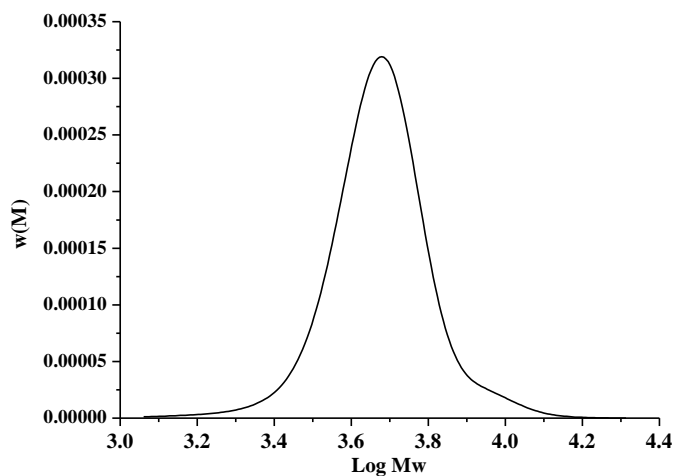


Figure S4: SEC trace of polymer **11**, determined from THF SEC, RI detector, PSTY standard, $M_n=4480$, $PDI=1.10$.

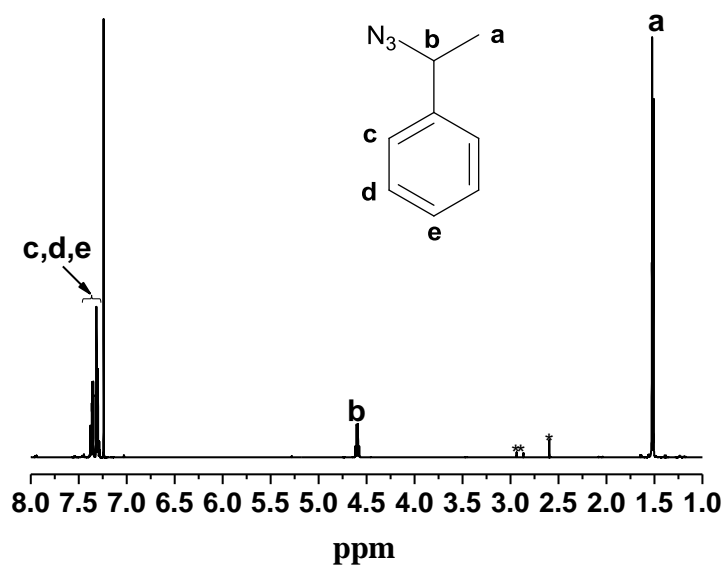


Figure S5: ^1H NMR spectrum (400 MHz) of (1-azidoethyl) benzene in CDCl_3 at 298 K, **=DMF. *=DMSO

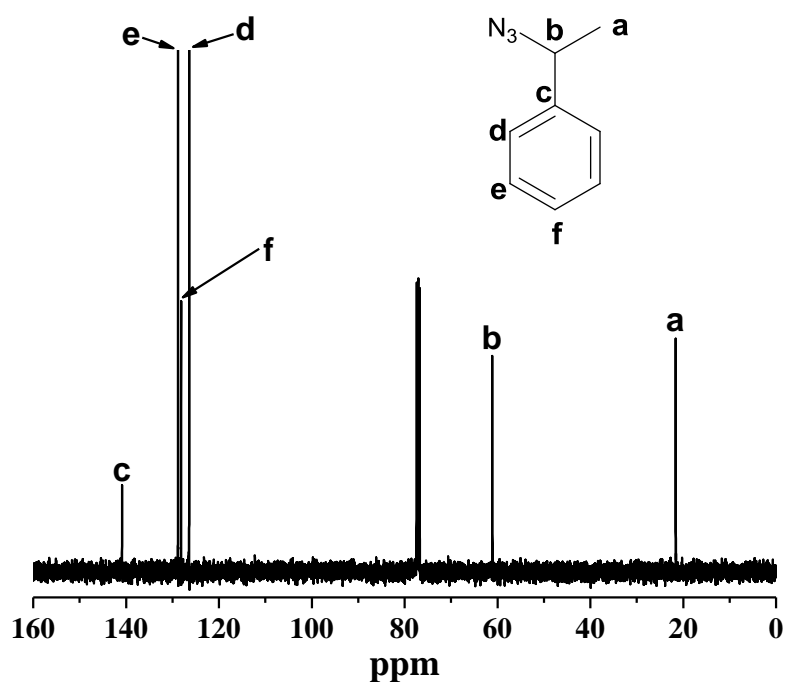


Figure S6: ^{13}C NMR spectrum (400 MHz) of (1-azidoethyl) benzene in CDCl_3 at 298 K.

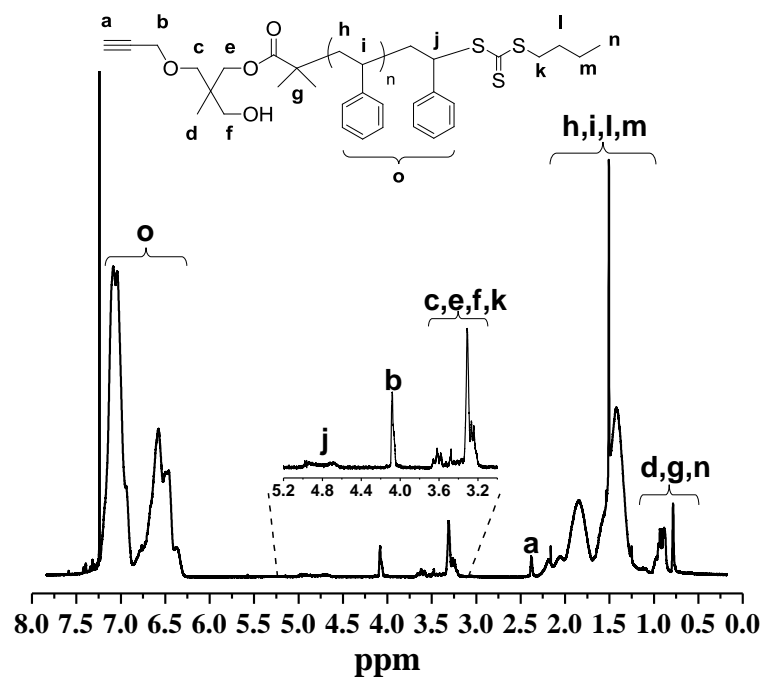


Figure S7: ^1H NMR spectrum (400 MHz) of **4a**, recorded in CDCl_3 at 298 K.

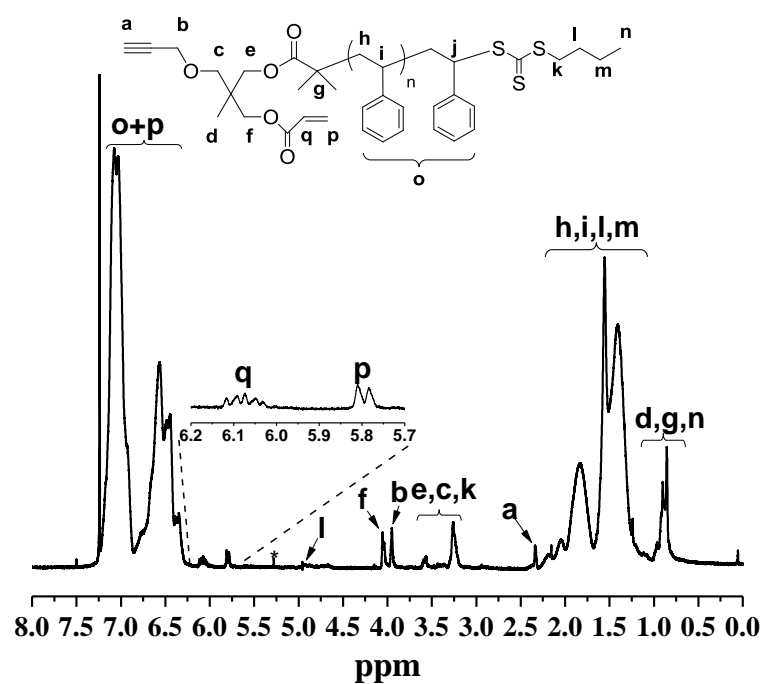


Figure S8: ^1H NMR spectrum (400 MHz) of **5a**, recorded in CDCl_3 at 298 K.

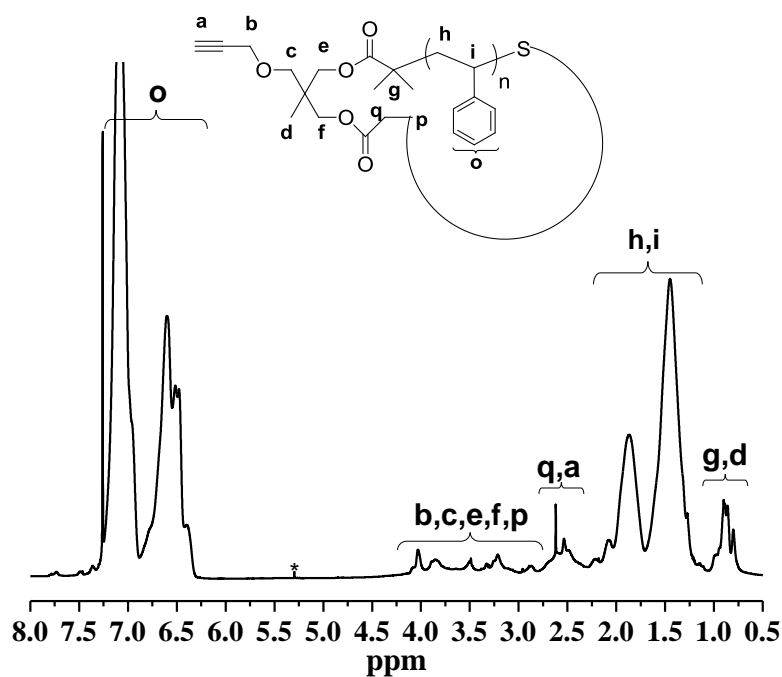


Figure S9: ^1H NMR spectrum (400 MHz) of **6a**, recorded in CDCl_3 at 298 K. *=DCM

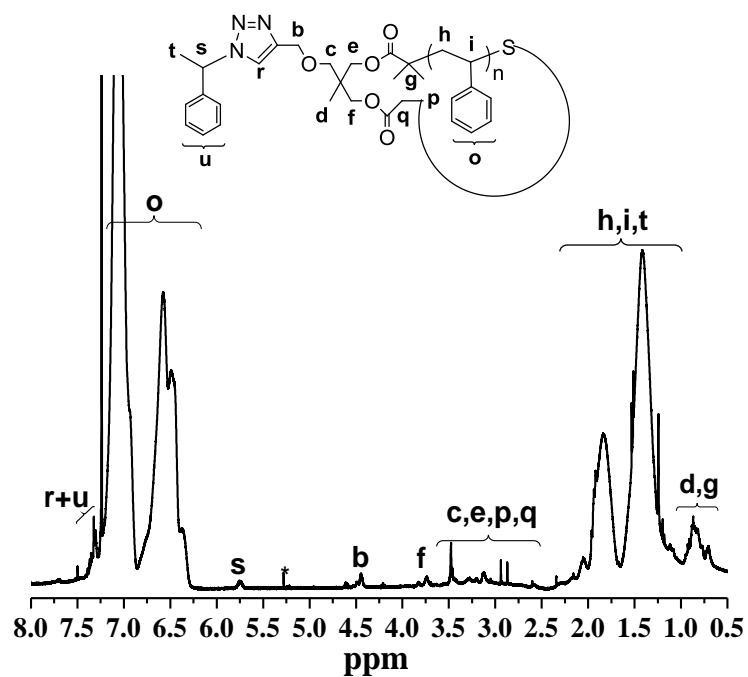


Figure S10: ^1H NMR spectrum (400 MHz) of **7a**, recorded in CDCl_3 at 298 K. *=DCM

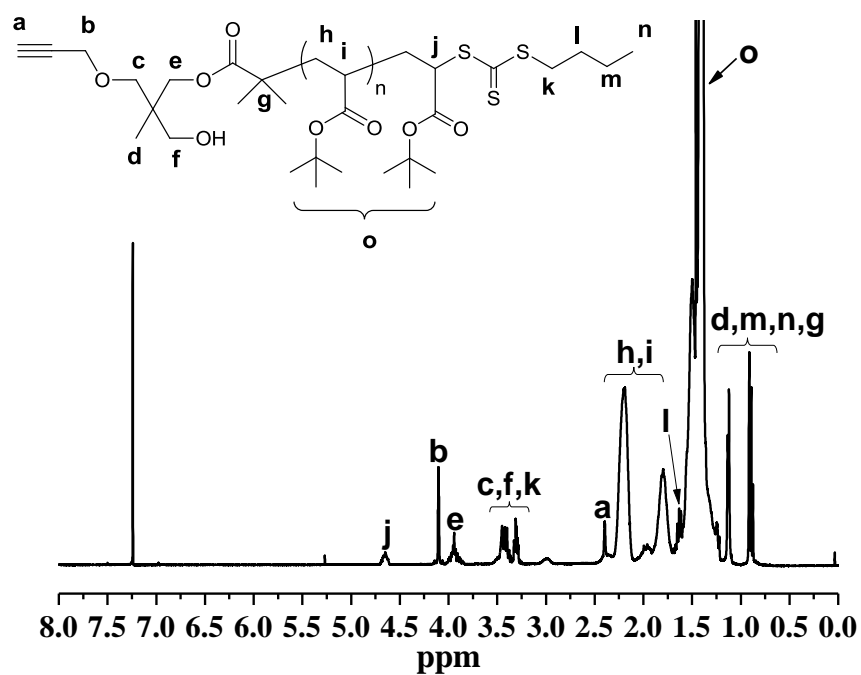


Figure S11: ^1H NMR spectrum (400 MHz) of **4b**, recorded in CDCl_3 at 298 K.

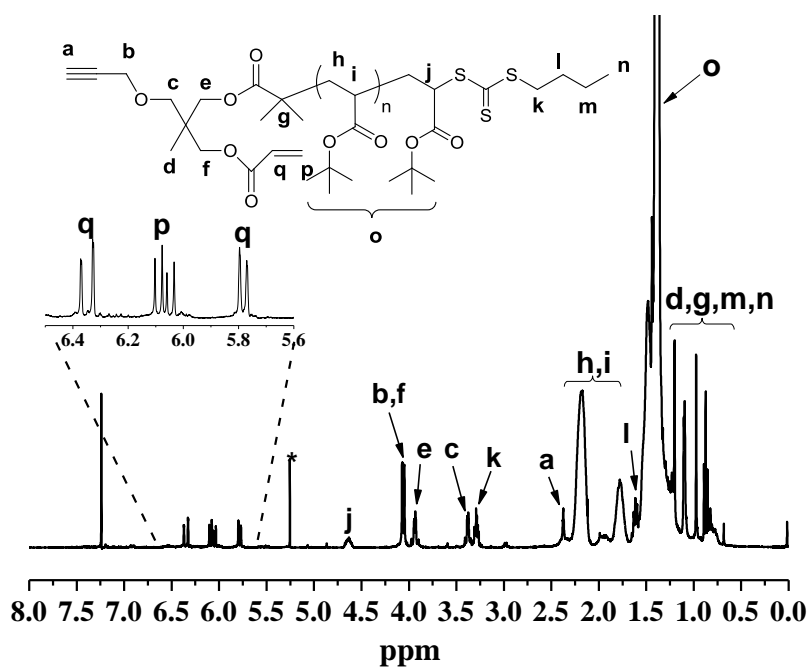


Figure S12: ^1H NMR spectrum (400 MHz) of **5b**, recorded in CDCl_3 at 298 K. *=DCM

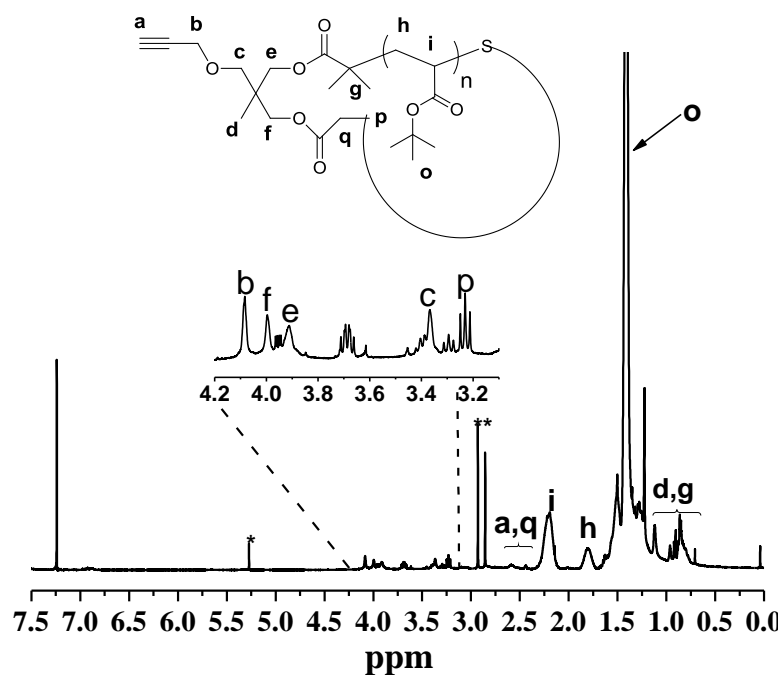


Figure S13: ^1H NMR spectrum (400 MHz) of **6b**, recorded in CDCl_3 at 298 K.*= DCM .

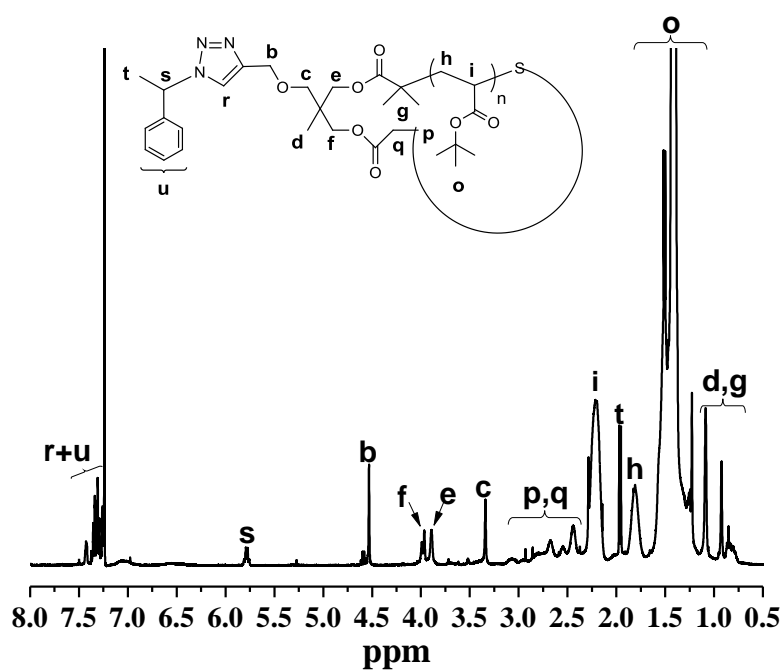


Figure S14: ^1H NMR spectrum (400 MHz) of **7b**, recorded in CDCl_3 at 298 K.

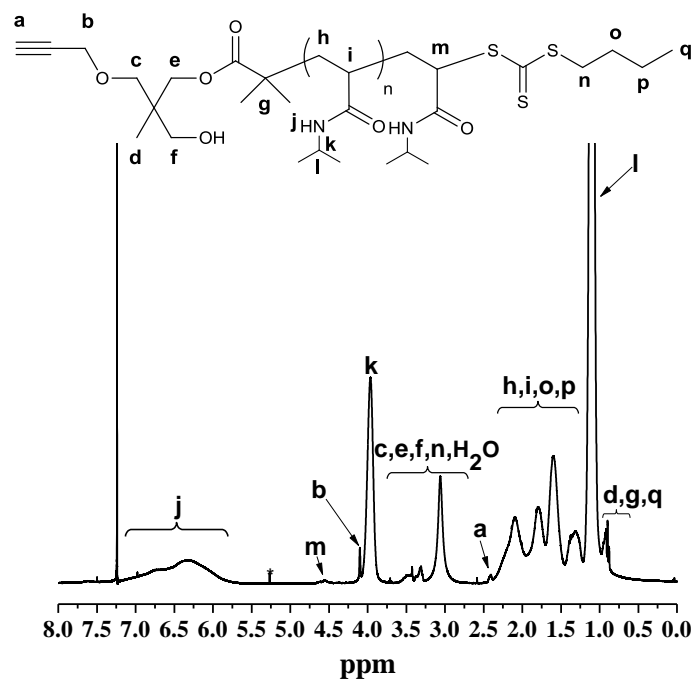


Figure S15: ^1H NMR spectrum (400 MHz) of **4c**, recorded in CDCl_3 at 298 K.

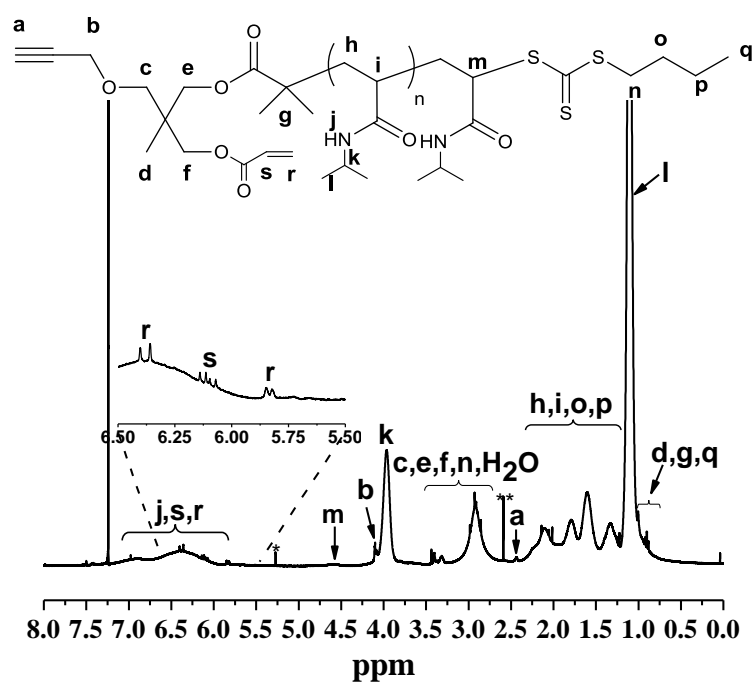


Figure S16: ^1H NMR spectrum (400 MHz) of **5c**, recorded in CDCl_3 at 298 K. *=DCM, **=DMSO.

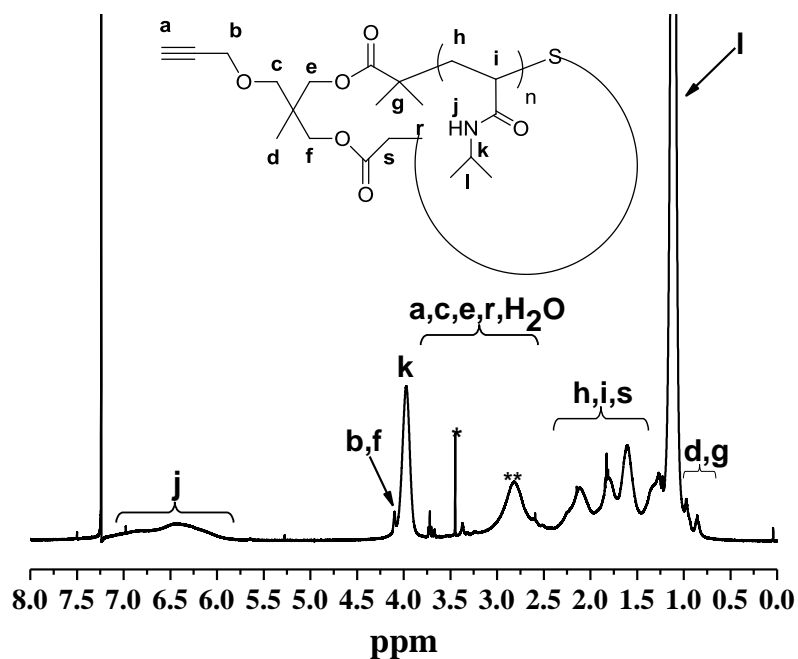


Figure S17: ^1H NMR spectrum (400 MHz) of **6c**, recorded in CDCl_3 at 298 K. *= Et_2O .

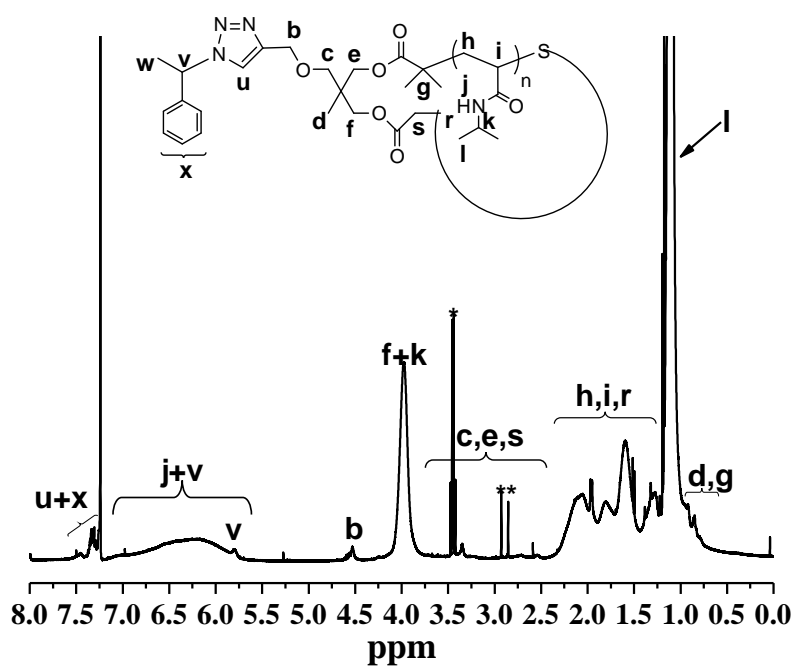


Figure S18: ^1H NMR spectrum (400 MHz) of **7c**, recorded in CDCl_3 at 298 K. *= Et_2O , **= DMF .

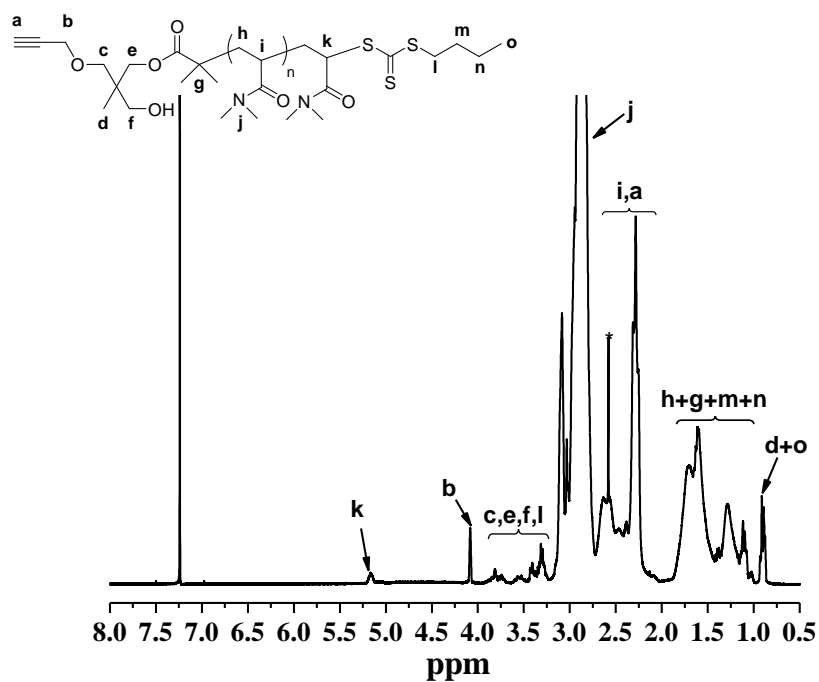


Figure S19: ^1H NMR spectrum (400 MHz) of **4d**, recorded in CDCl_3 at 298 K.

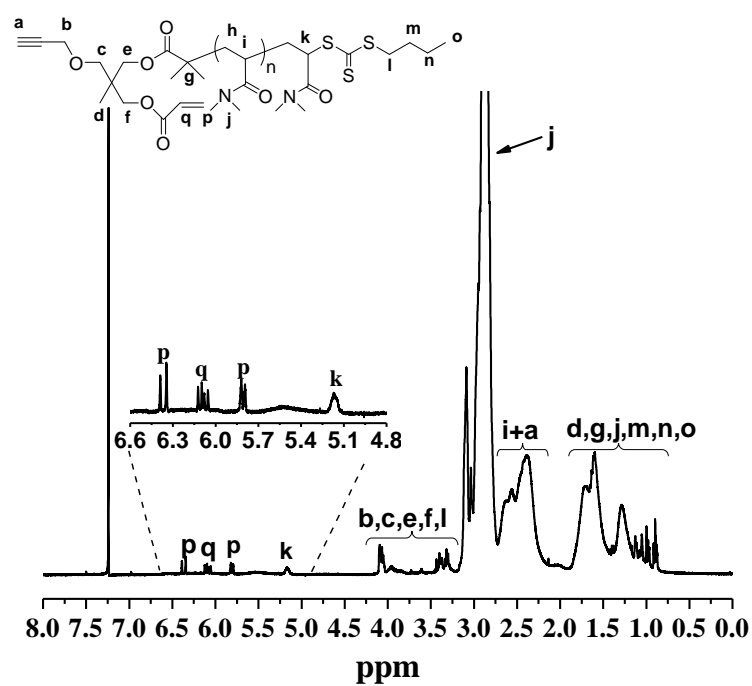


Figure S20: ^1H NMR spectrum (400 MHz) of **5d**, recorded in CDCl_3 at 298 K.

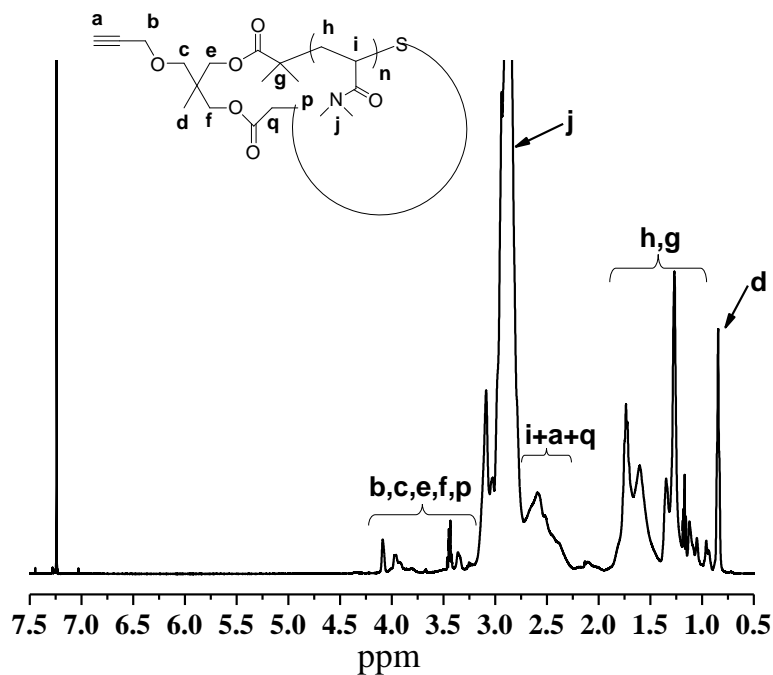


Figure S21: ^1H NMR spectrum (400 MHz) of **6d**, recorded in CDCl_3 at 298 K.

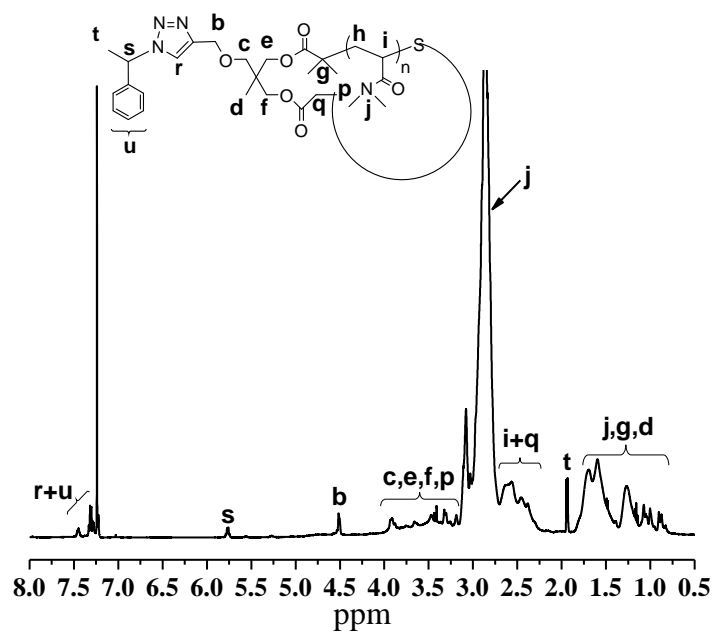


Figure S22: ^1H NMR spectrum (400 MHz) of **7d**, recorded in CDCl_3 at 298 K.

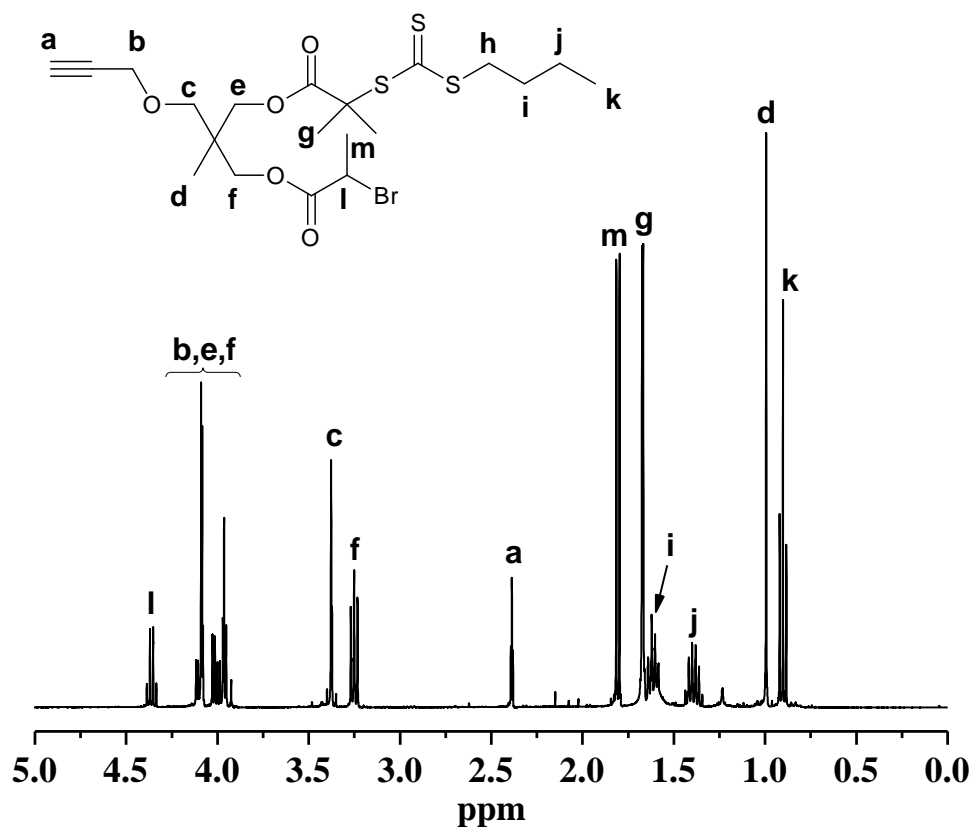


Figure S23: ^1H NMR spectrum (400 MHz) of **10**, recorded in CDCl_3 at 298 K.

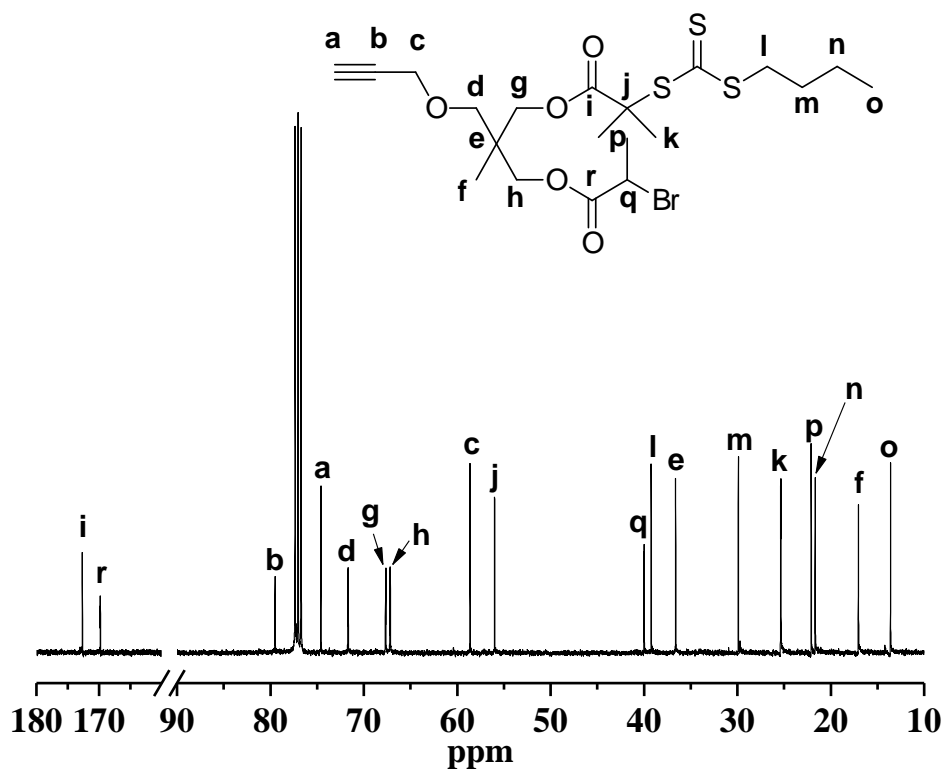


Figure S24: ^{13}C NMR spectrum (400 MHz) of **10**, recorded in CDCl_3 at 298 K.

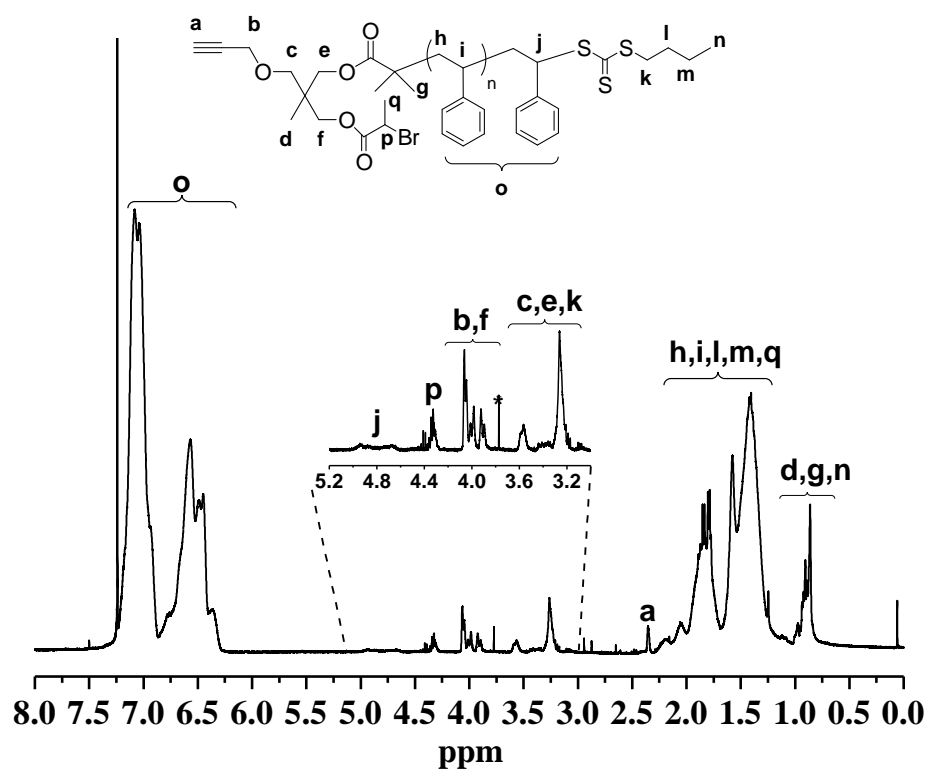


Figure S25: ¹H NMR spectrum (400 MHz) of **8**, recorded in CDCl₃ at 298 K.

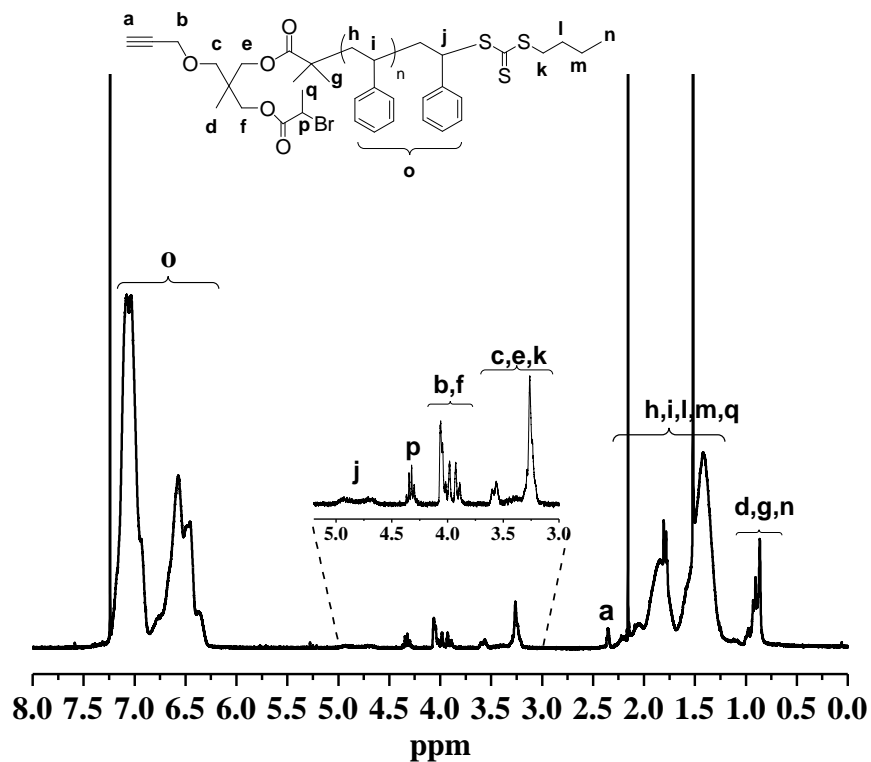


Figure S26: ¹H NMR spectrum (400 MHz) of **11**, recorded in CDCl₃ at 298 K.

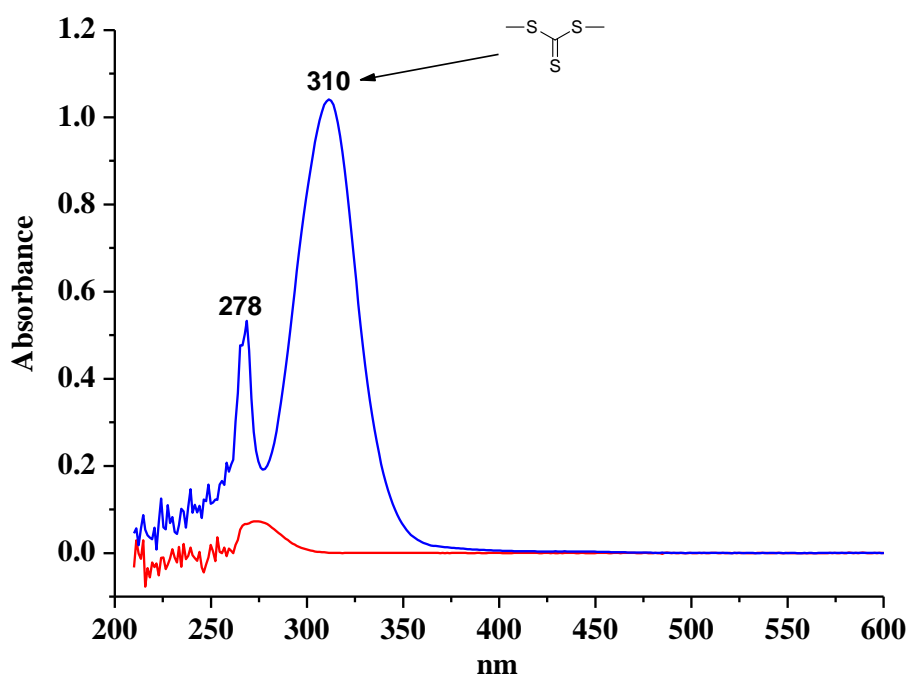


Figure S27: UV-vis absorbance of **5a** (blue) and **6a** (red). UV-vis spectrum was recorded by UV-detector of THF GPC with the same concentration of polymers. The peak at 310 nm is attributed to RAFT moiety.

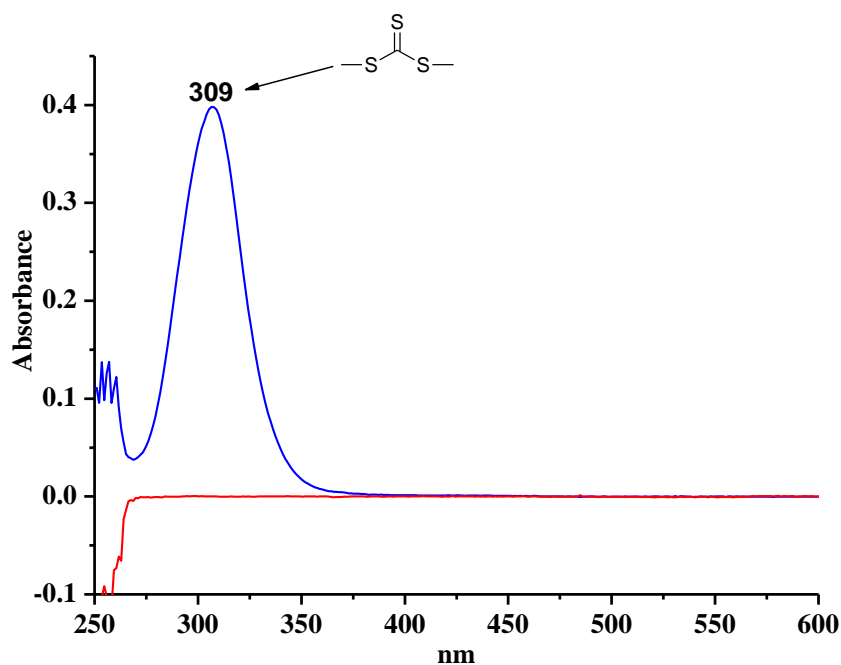


Figure S28: UV-vis absorbance of **5b** (blue) and **6b** (red). UV-vis spectrum was recorded by UV-detector of THF GPC with the same concentration of polymers. The peak at 309 nm is attributed to RAFT moiety.

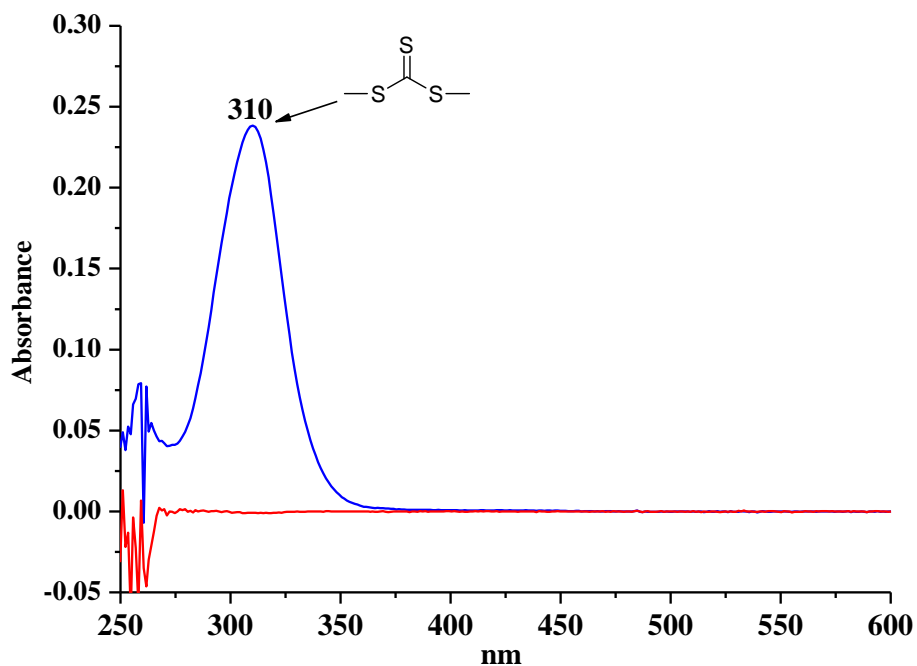


Figure S29: UV-Vis absorbance of **5c** (blue) and **6c** (red). UV-vis spectrum was recorded by UV-detector of THF GPC with the same concentration of polymers. The peak at 310 nm is attributed to RAFT moiety.

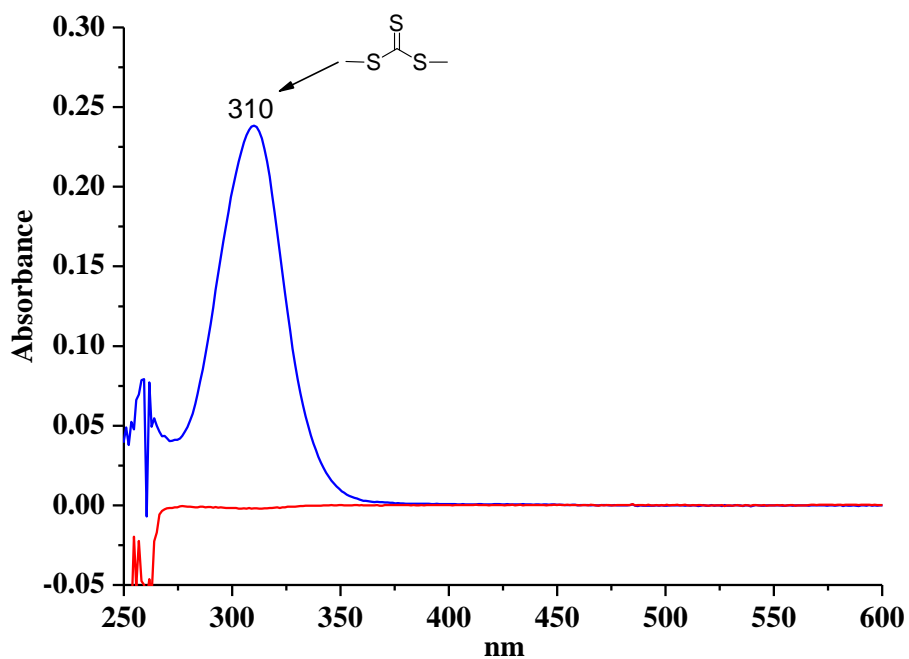


Figure S30: UV-vis absorbance of **5d** (blue) and **6d** (red). UV-vis spectrum was recorded by UV-detector of THF GPC with the same concentration of polymers. The peak at 310 nm is attributed to RAFT moiety.

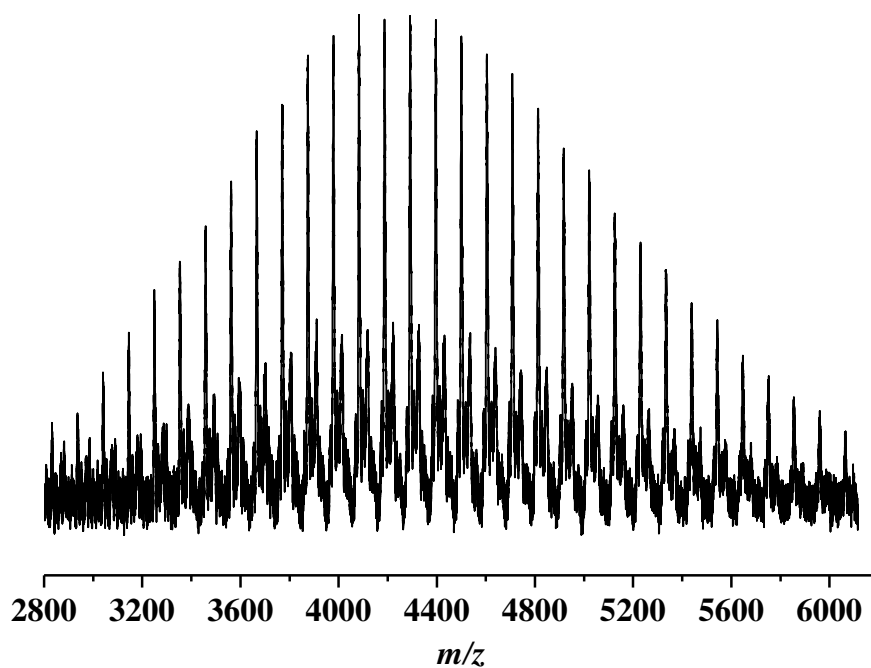


Figure S31: Full MALDI-ToF mass spectrum of **4a** with $\text{Ag}(\text{CF}_3\text{COO})$ as cationization agent from a DCTB matrix in reflectron mode.

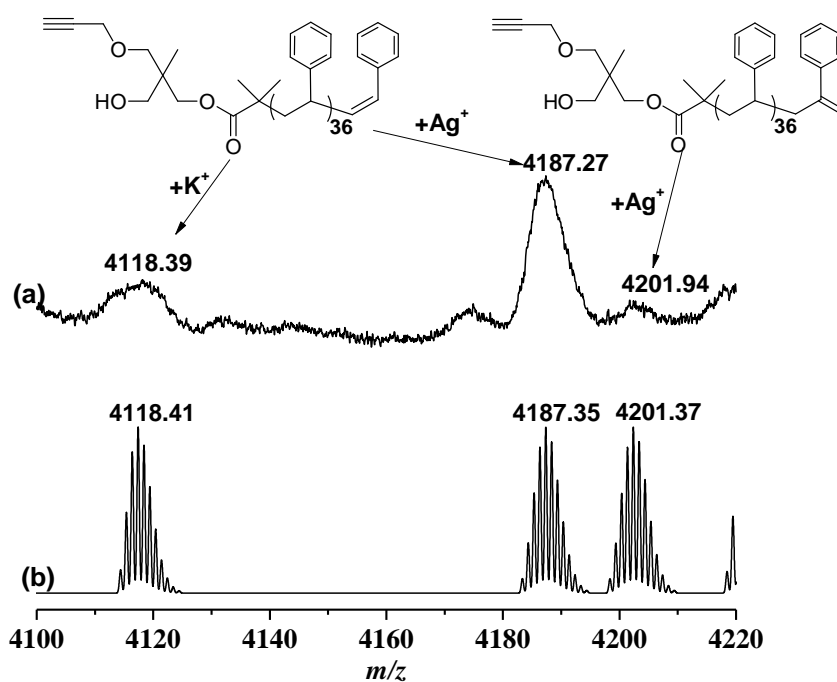


Figure S32: Expanded MALDI-ToF mass spectrum of **4a** with $\text{Ag}(\text{CF}_3\text{COO})$ as cationization agent from a DCTB matrix in reflectron mode. (a) experimental isotopic resolution of peaks (b) theoretical isotopic pattern of products.

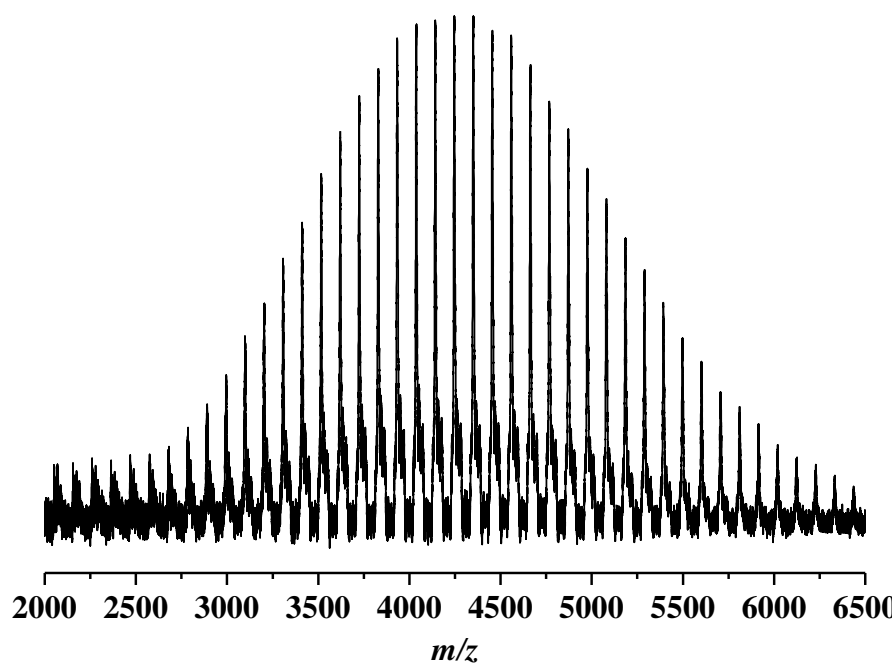


Figure S33: Full MALDI-ToF mass spectrum of **5a** with $\text{Ag}(\text{CF}_3\text{COO})$ as cationization agent from a DCTB matrix in reflectron mode.

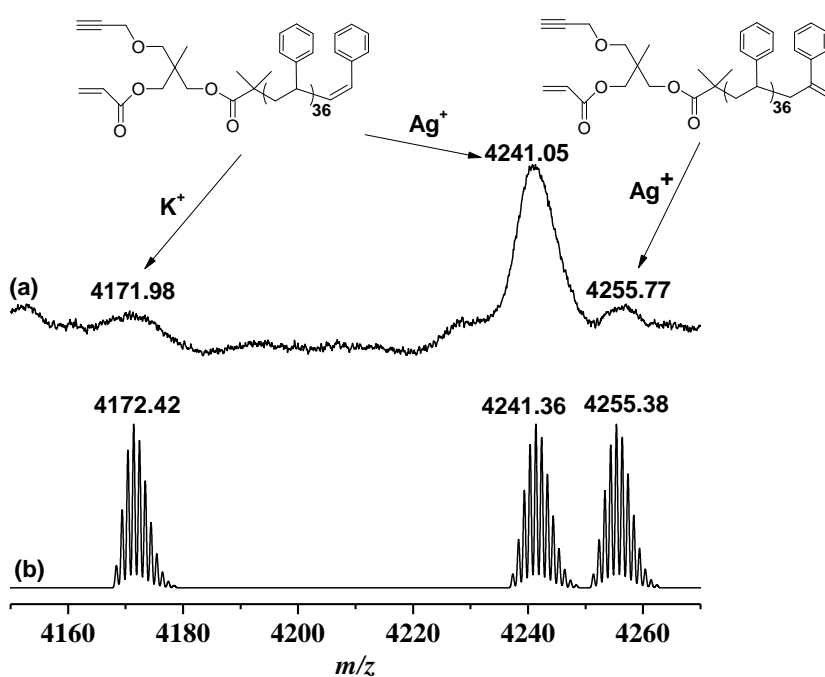


Figure S34: Expanded MALDI-ToF mass spectrum of **5a** with $\text{Ag}(\text{CF}_3\text{COO})$ as cationization agent from a DCTB matrix in reflectron mode. (a) experimental isotopic resolution of peaks (b) theoretical isotopic pattern of products.

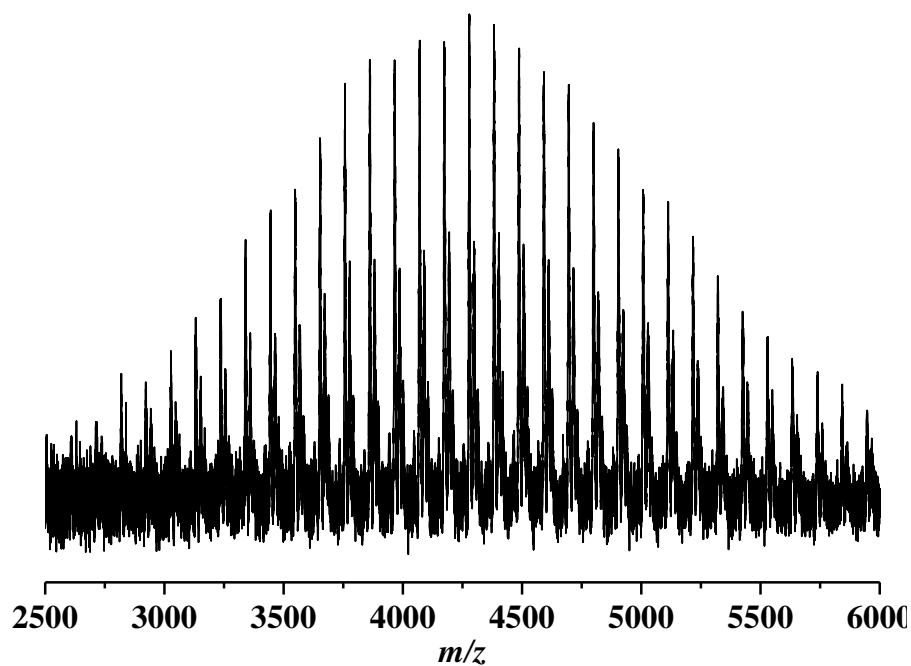


Figure S35: Full MALDI-ToF mass spectrum of **6a** with $\text{Ag}(\text{CF}_3\text{COO})$ as cationization agent from a DCTB matrix in reflectron mode.

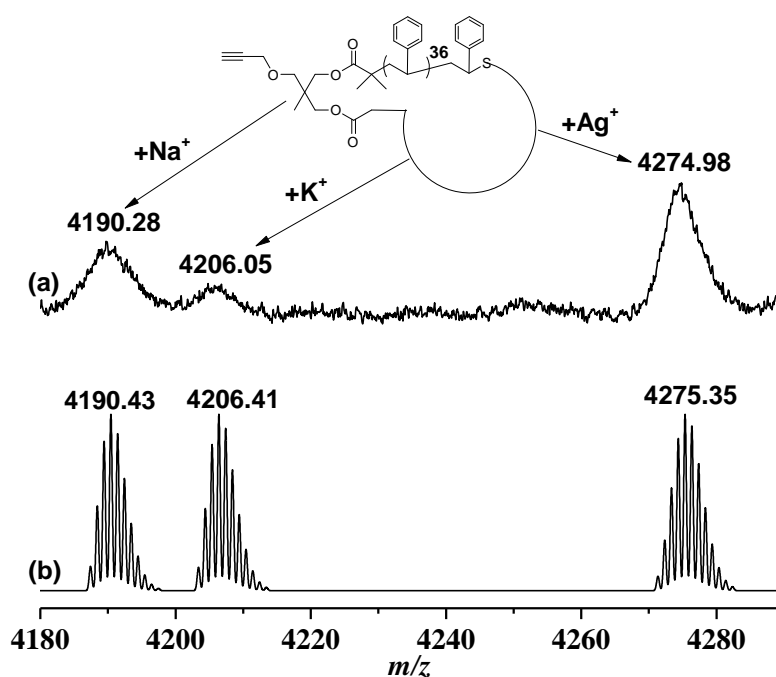


Figure S36: Expanded MALDI-ToF mass spectrum of **6a** with $\text{Ag}(\text{CF}_3\text{COO})$ as cationization agent from a DCTB matrix in reflectron mode. (a) experimental isotopic resolution of peaks (b) theoretical isotopic pattern of products.

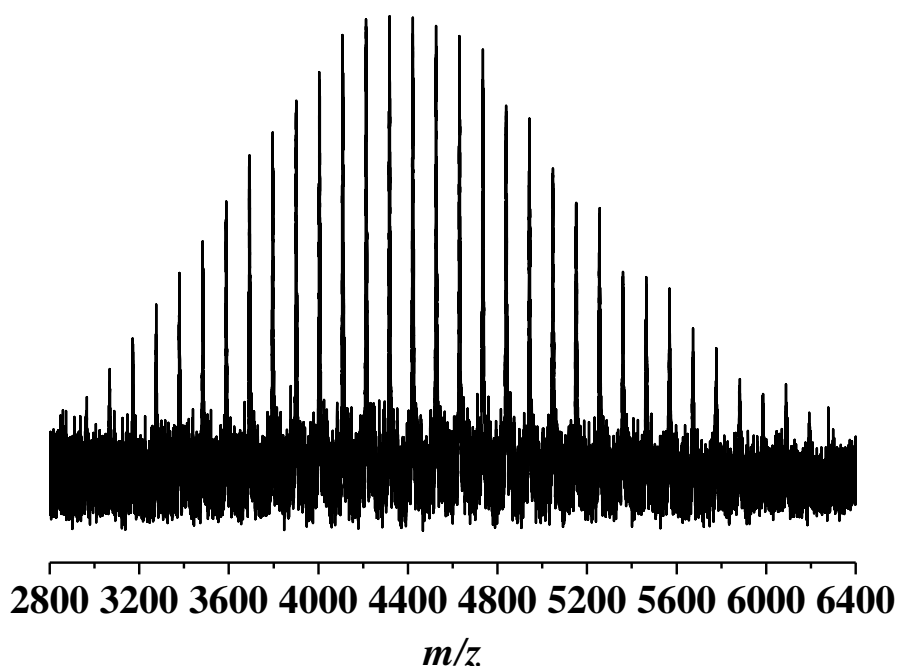


Figure S37: Full MALDI-ToF mass spectrum of **7a** with Ag(CF₃COO) as cationization agent from a DCTB matrix in reflectron mode.

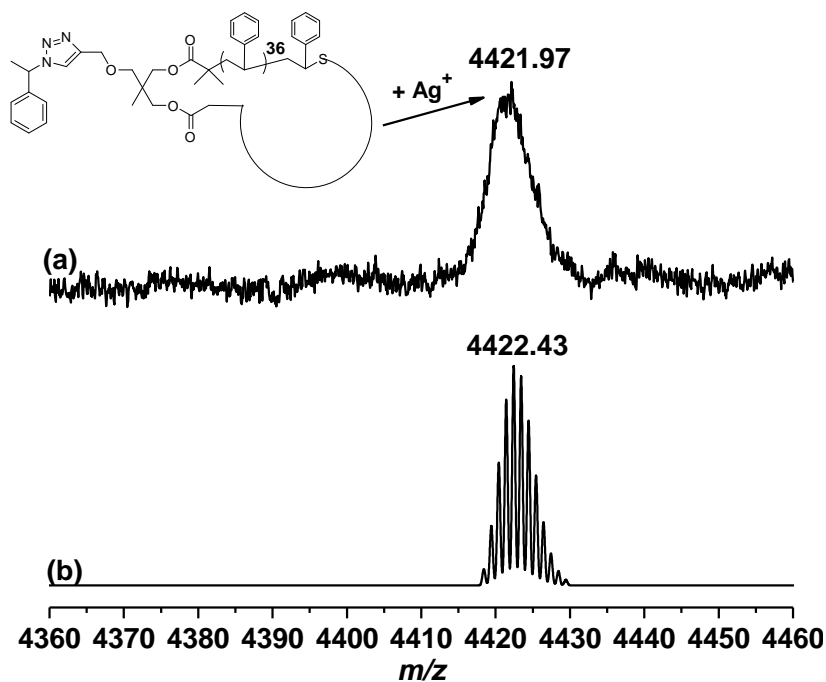


Figure S38: Expanded MALDI-ToF mass spectrum of **7a** with Ag(CF₃COO) as cationization agent from a DCTB matrix in reflectron mode. (a) experimental isotopic resolution of peaks (b) theoretical isotopic pattern of products.

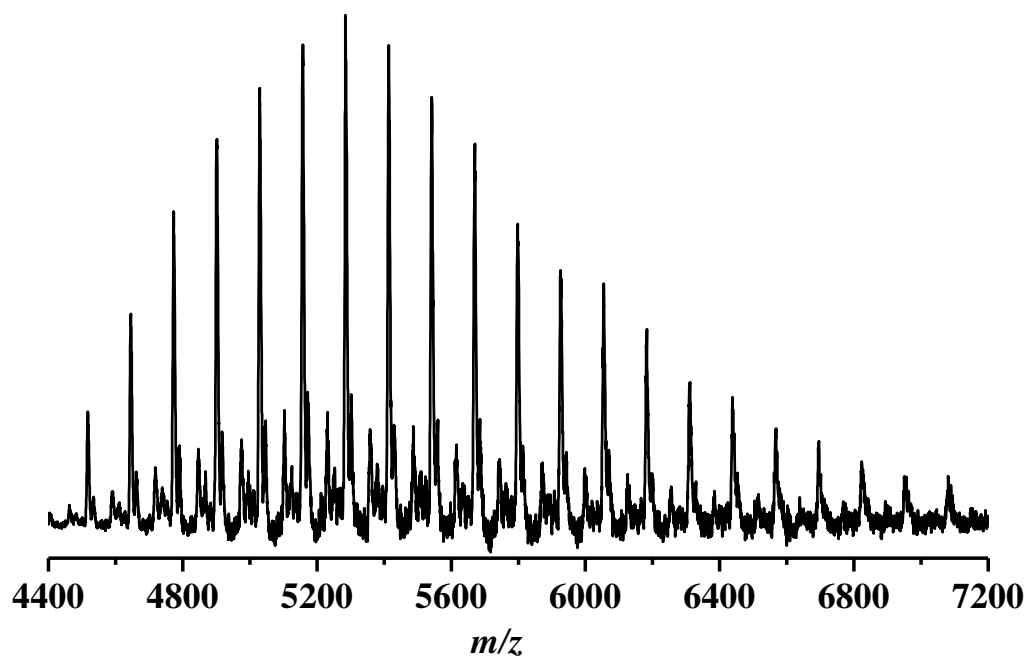


Figure S39: Full MALDI-ToF mass spectrum of **4b** with Na(CF₃COO) as cationization agent from a DCTB matrix in linear mode.

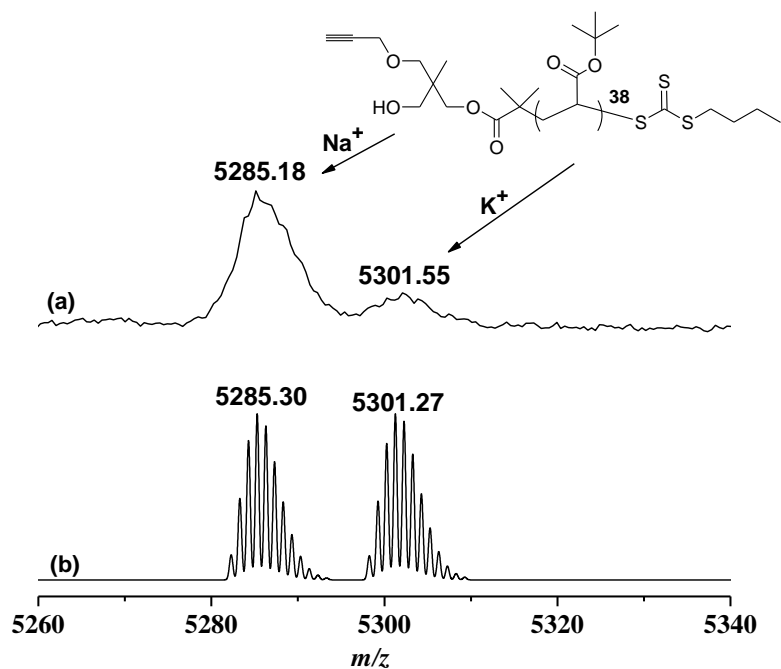


Figure S40: Expanded MALDI-ToF mass spectrum of **4b** with Na(CF₃COO) as cationization agent from a DCTB matrix in linear mode. (a) experimental isotopic resolution of peaks (b) theoretical isotopic pattern of products.

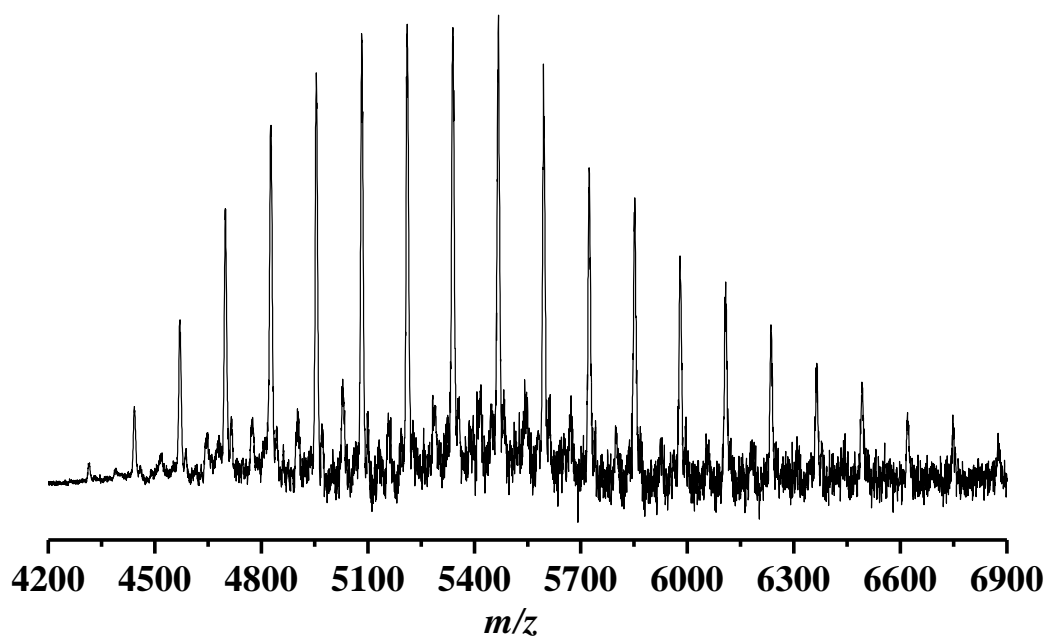


Figure S41: Full MALDI-ToF mass spectrum of **5b** with Na(CF₃COO) as cationization agent from a DCTB matrix in linear mode.

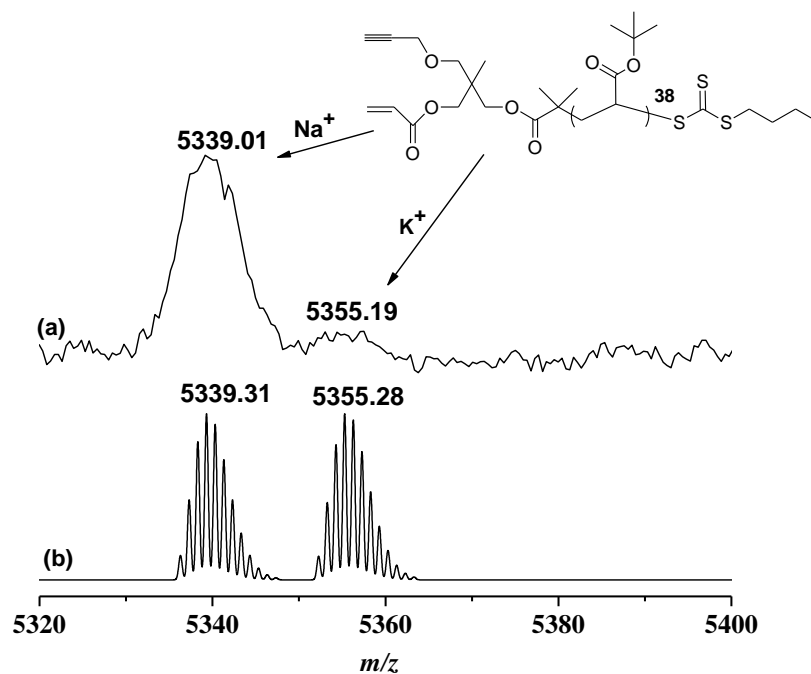


Figure S42: Expanded MALDI-ToF mass spectrum of **5b** with Na(CF₃COO) as cationization agent from a DCTB matrix in linear mode. (a) experimental isotopic resolution of peaks (b) theoretical isotopic pattern of products.

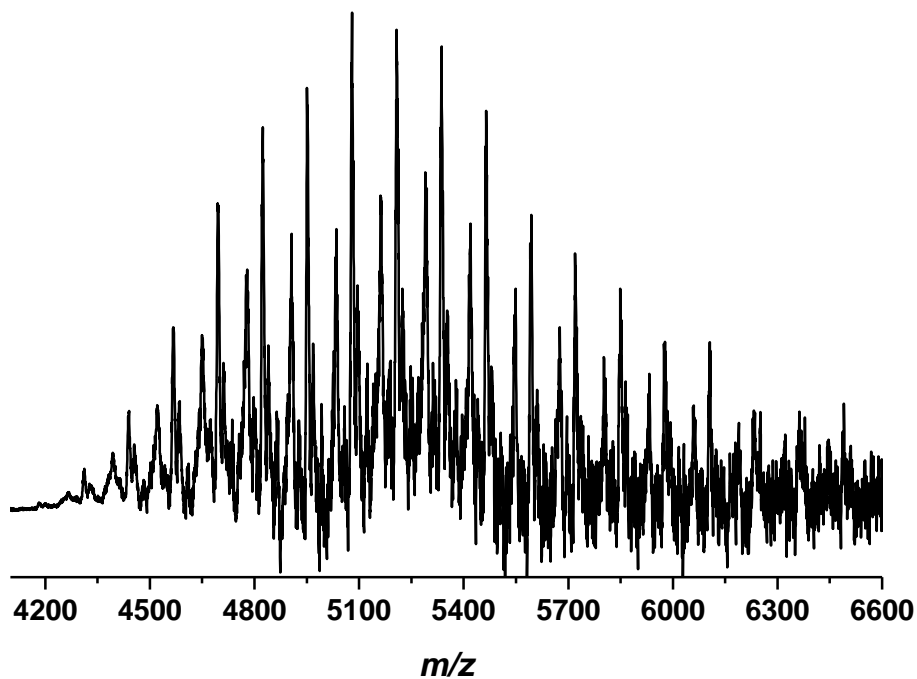


Figure S43: Full MALDI-ToF mass spectrum of **6b** with Na(CF₃COO) as cationization agent from a DCTB matrix in linear mode.

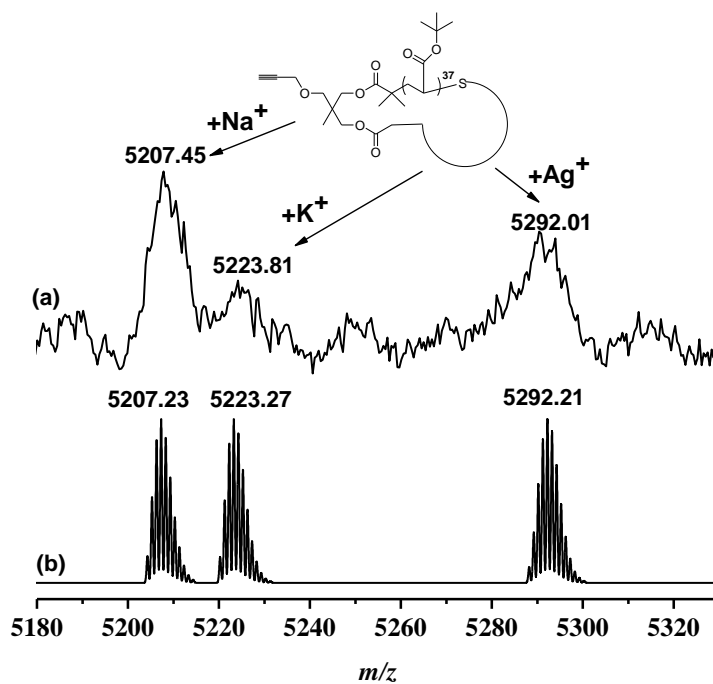


Figure S44: Expanded MALDI-ToF mass spectrum of **6b** with Na(CF₃COO) as cationization agent from a DCTB matrix in reflectron mode. (a) experimental isotopic resolution of peaks (b) theoretical isotopic pattern of products.

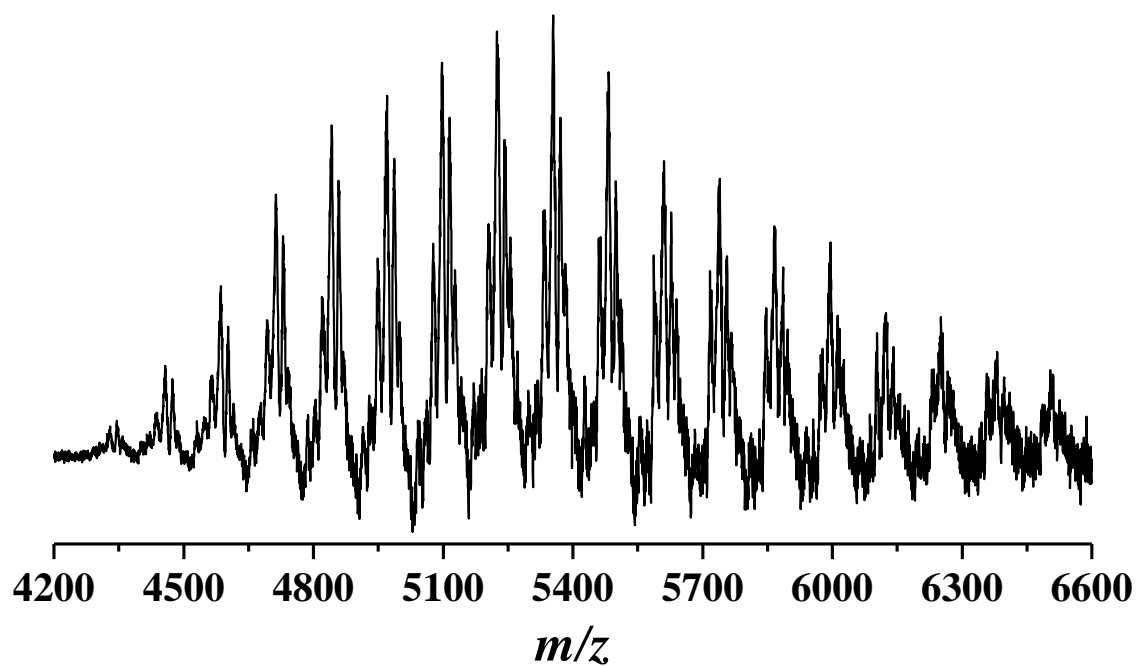


Figure S45: Full MALDI-ToF mass spectrum of **7b** with Na(CF₃COO) as cationization agent from a DCTB matrix in linear mode.

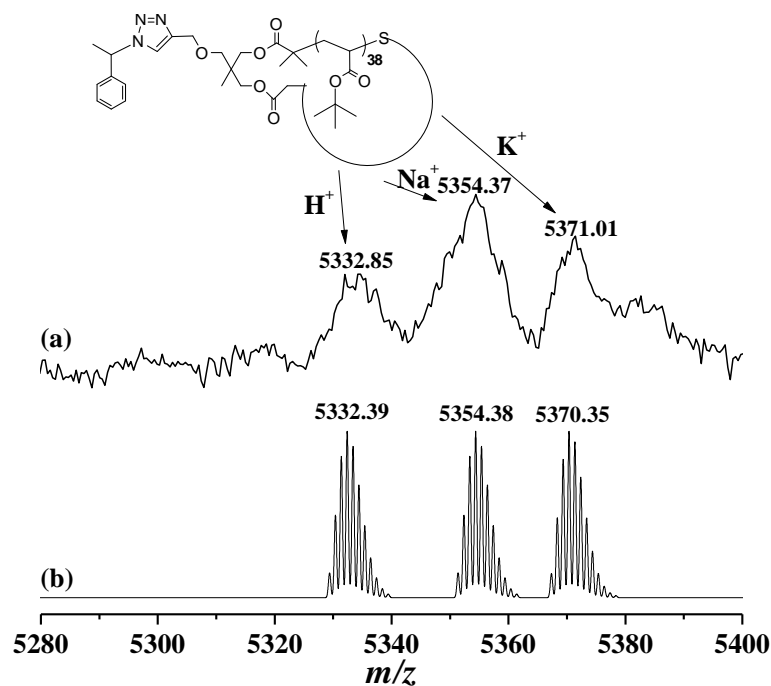


Figure S46: Expanded MALDI-ToF mass spectrum of **7b** with Na(CF₃COO) as cationization agent from a DCTB matrix in linear mode. (a) experimental isotopic resolution of peaks (b) theoretical isotopic pattern of products.

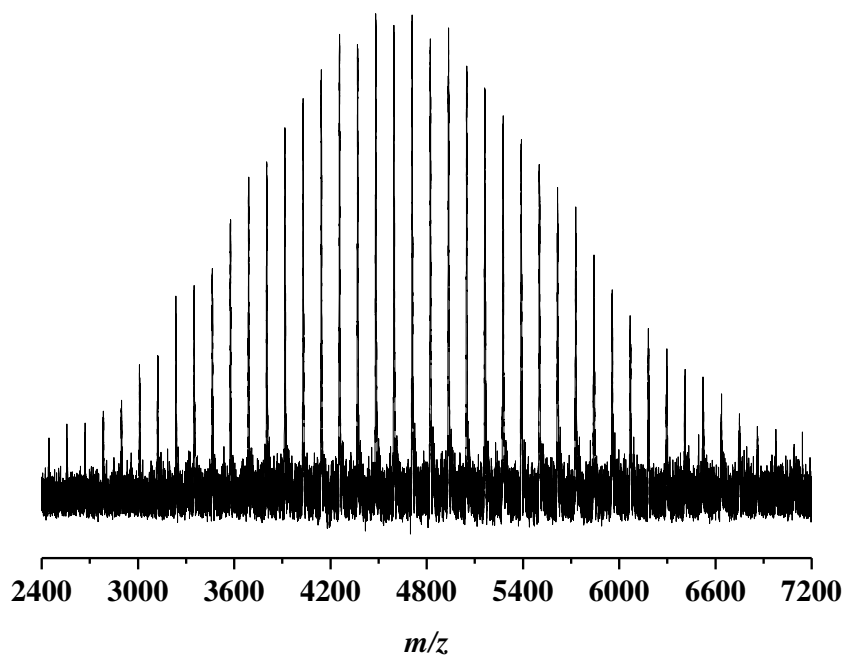


Figure S47: Full MALDI-ToF mass spectrum of **4c** with Na(CF₃COO) as cationization agent from a DCTB matrix in reflectron mode.

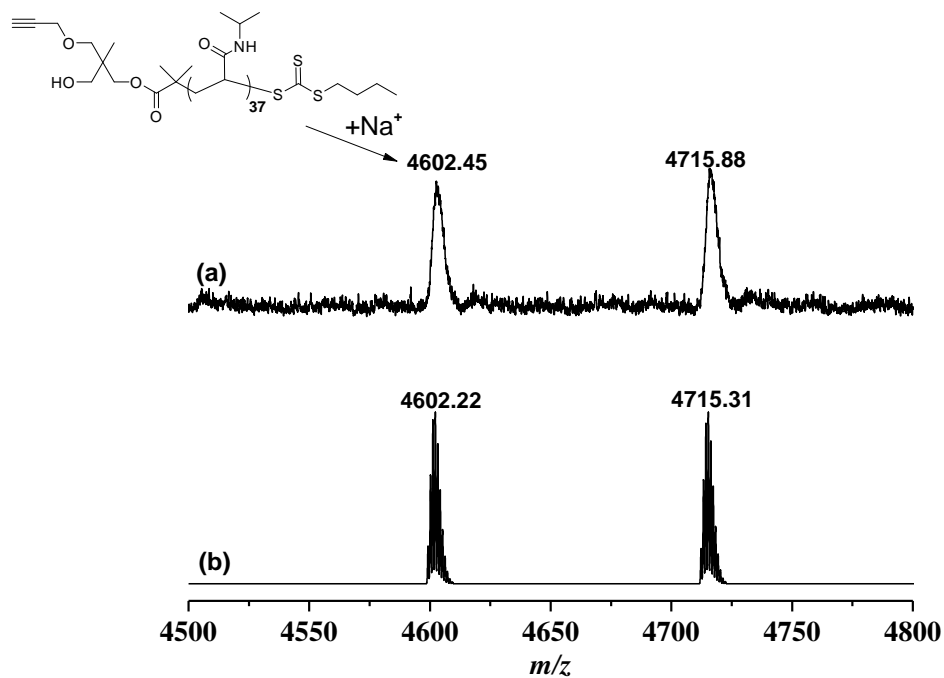


Figure S48: Expanded MALDI-ToF mass spectrum of **4c** with Na(CF₃COO) as cationization agent from a DCTB matrix in reflectron mode. (a) experimental isotopic resolution of peaks (b) theoretical isotopic pattern of products.

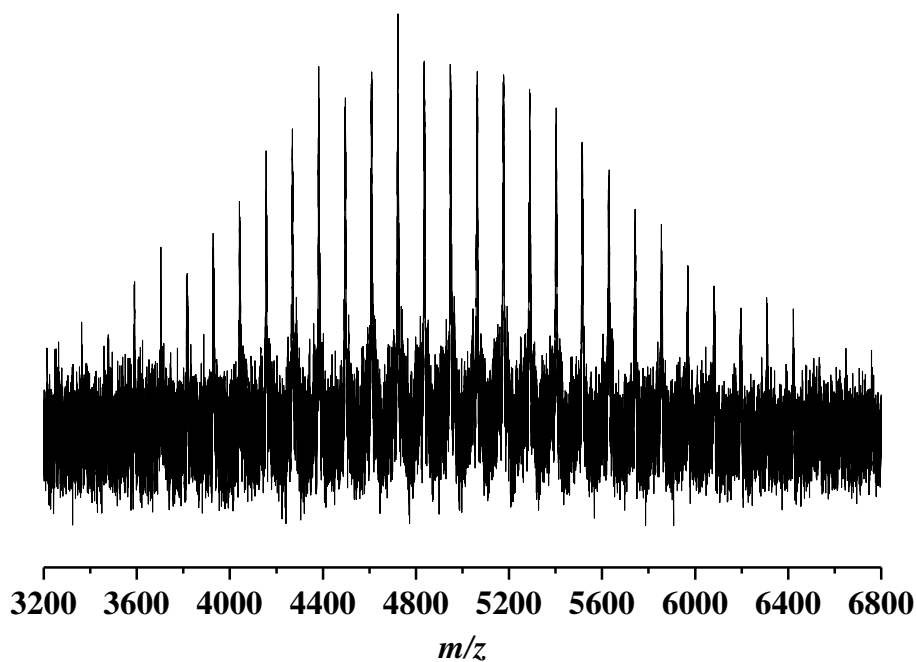


Figure S49: Full MALDI-ToF mass spectrum of **5c** with Na(CF₃COO) as cationization agent from a DCTB matrix in reflectron mode.

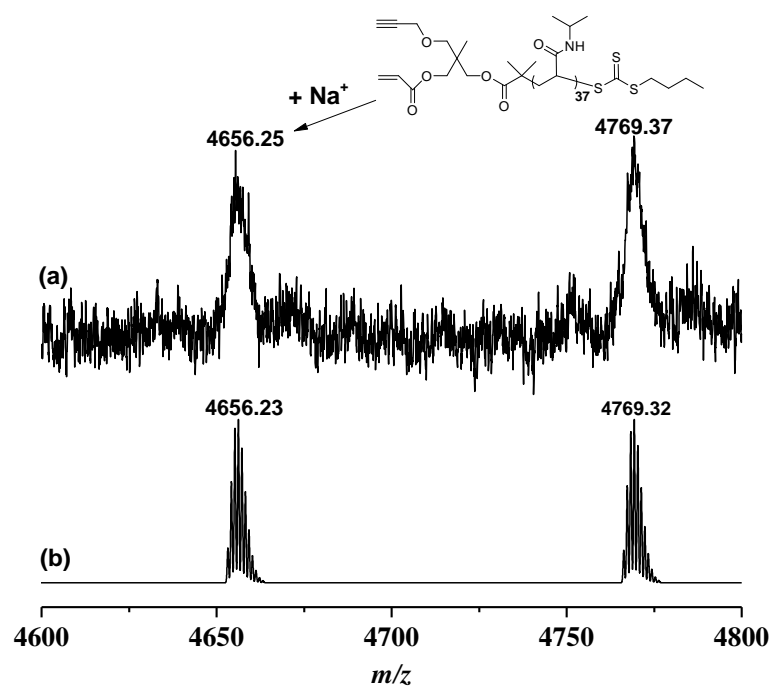


Figure S50: Expanded MALDI-ToF mass spectrum of **5c** with Na(CF₃COO) as cationization agent from a DCTB matrix in reflectron mode. (a) experimental isotopic resolution of peaks (b) theoretical isotopic pattern of products.

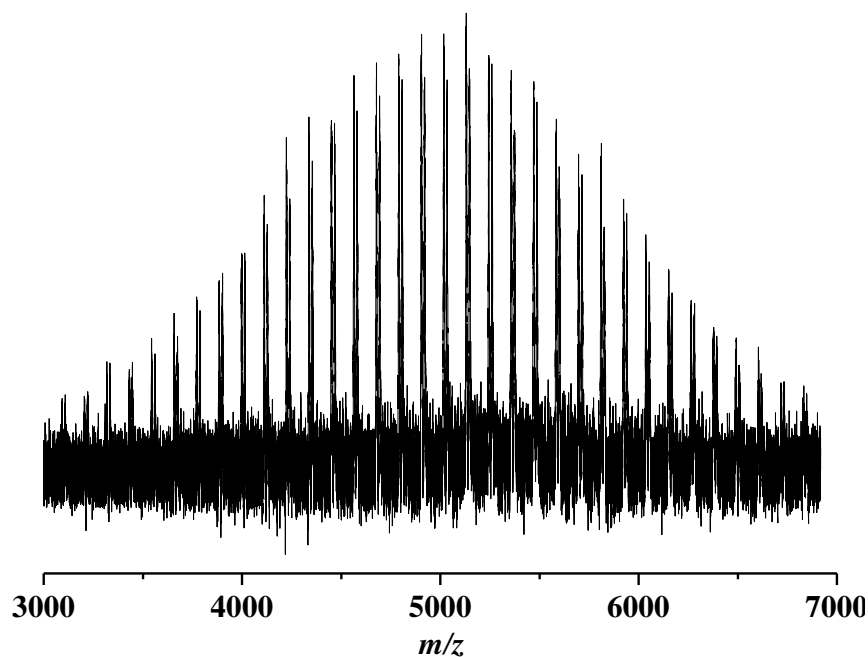


Figure S51: Full MALDI-ToF mass spectrum of **6c** with Na(CF₃COO) as cationization agent from a DCTB matrix in reflectron mode.

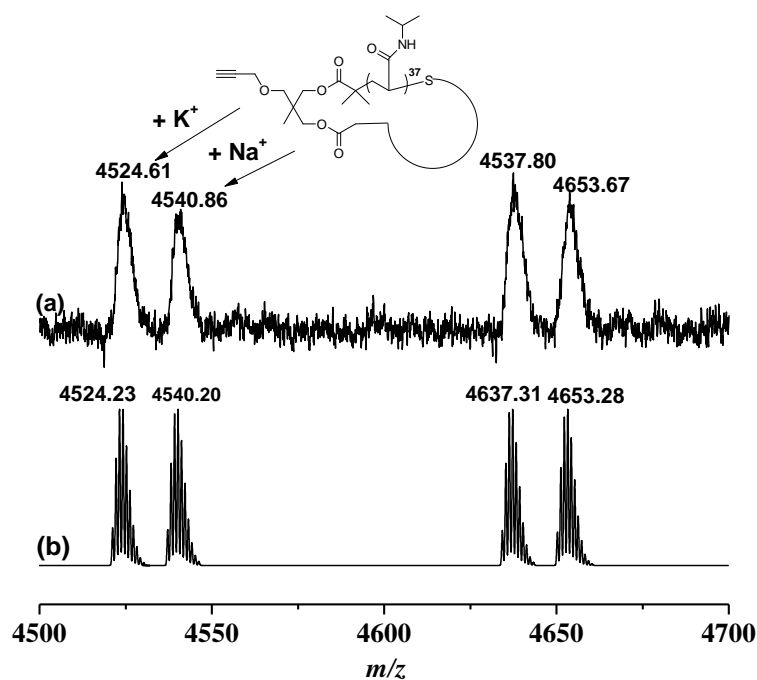


Figure S52: Expanded MALDI-ToF mass spectrum of **6c** with Na(CF₃COO) as cationization agent from a DCTB matrix in reflectron mode. (a) experimental isotopic resolution of peaks (b) theoretical isotopic pattern of products.

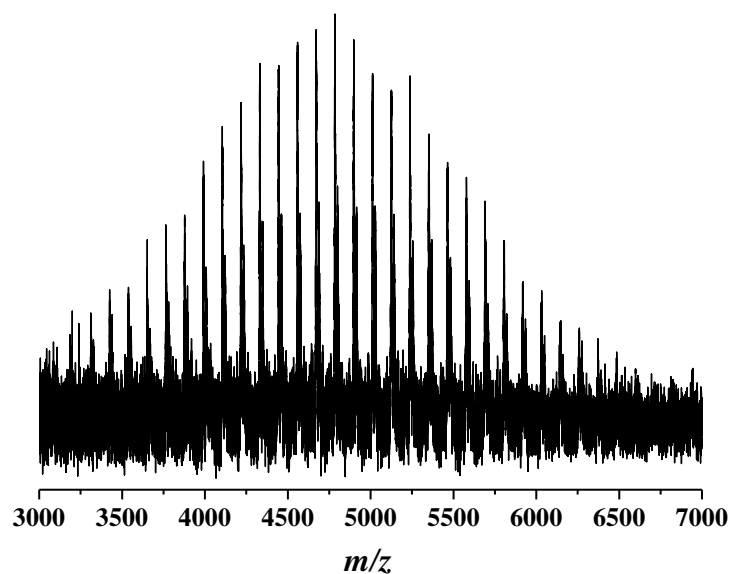


Figure S53: Full MALDI-ToF mass spectrum of **7c** with Na(CF₃COO) as cationization agent from a DCTB matrix in reflectron mode.

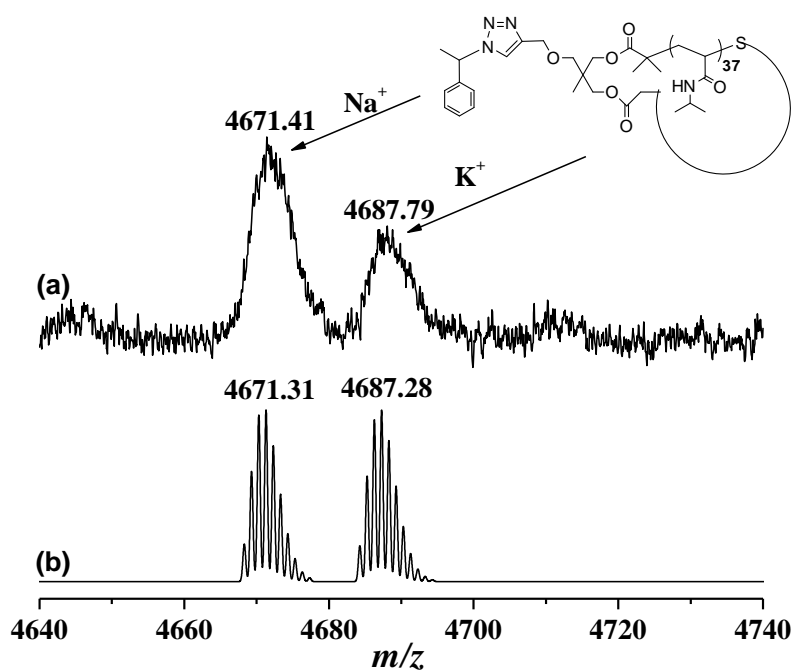


Figure S54: Expanded MALDI-ToF mass spectrum of **7c** with Na(CF₃COO) as cationization agent from a DCTB matrix in reflectron mode. (a) experimental isotopic resolution of peaks (b) theoretical isotopic pattern of products.

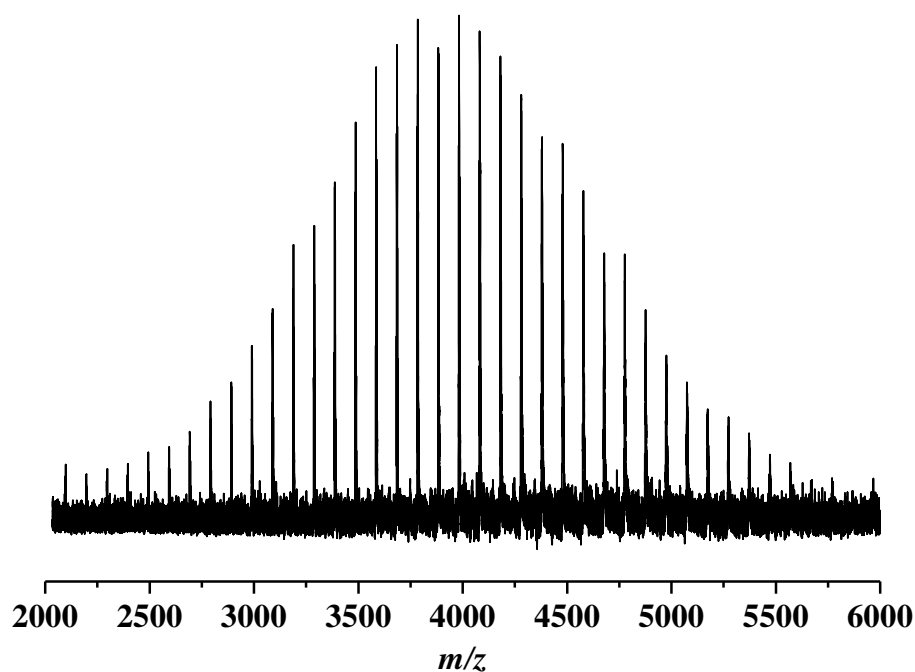


Figure S55: Full MALDI-ToF mass spectrum of **4d** with Na(CF₃COO) as cationization agent from a DCTB matrix in reflectron mode.

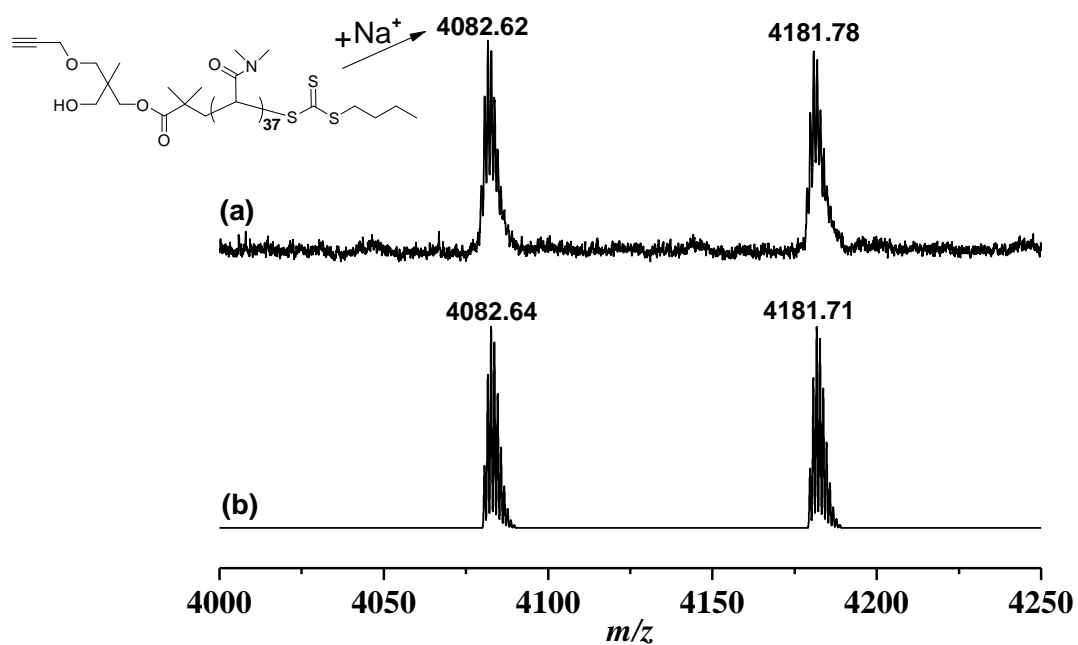


Figure S56: Expanded MALDI-ToF mass spectrum of **4d** with Na(CF₃COO) as cationization agent from a DCTB matrix in reflectron mode. (a) experimental isotopic resolution of peaks (b) theoretical isotopic pattern of products.

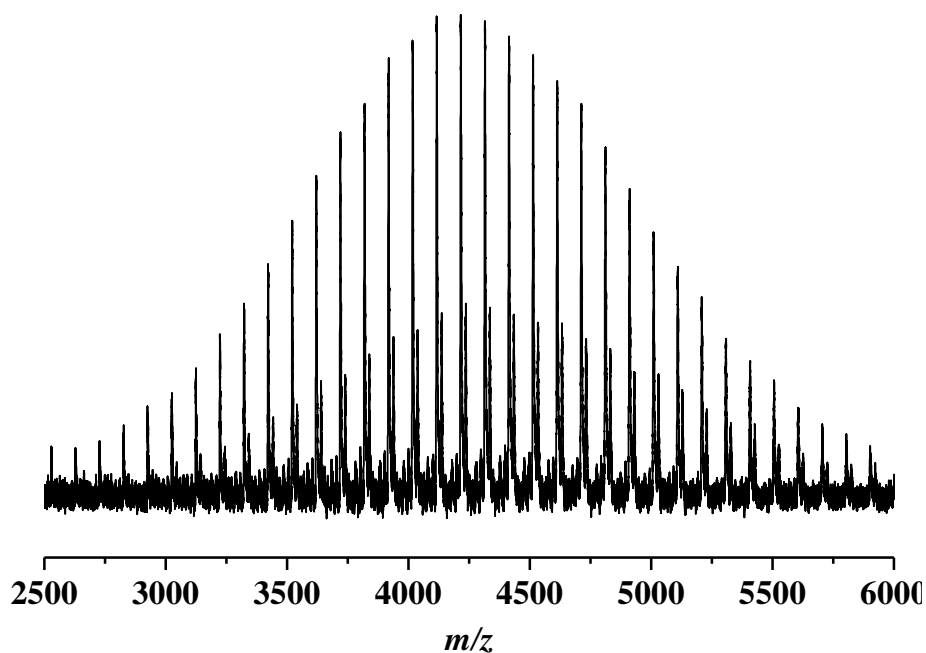


Figure S57: Full MALDI-ToF mass spectrum of **5d** with Na(CF₃COO) as cationization agent from a DCTB matrix in reflectron mode.

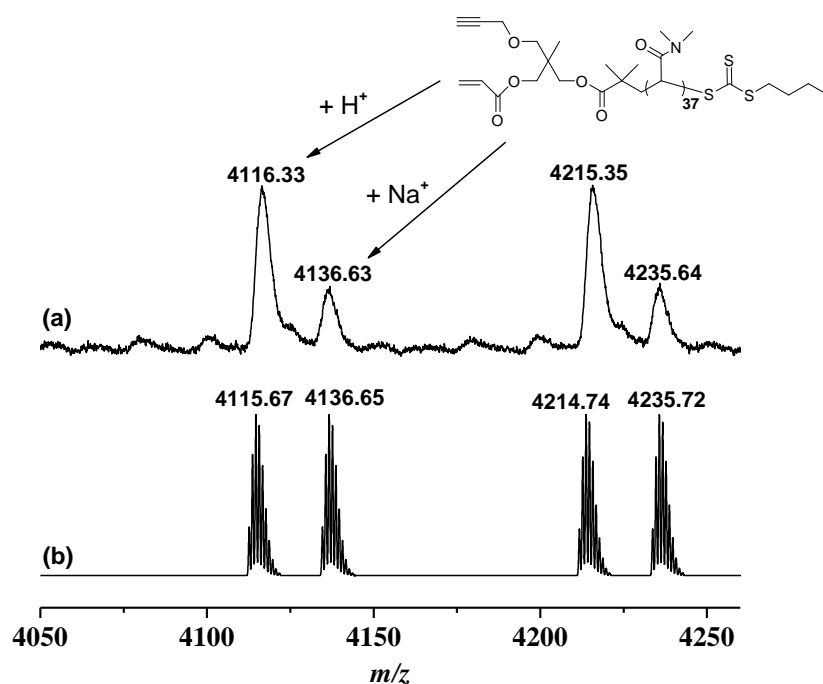


Figure S58: Expanded MALDI-ToF mass spectrum of **5d** with Na(CF₃COO) as cationization agent from a DCTB matrix in reflectron mode. (a) experimental isotopic resolution of peaks (b) theoretical isotopic pattern of products.

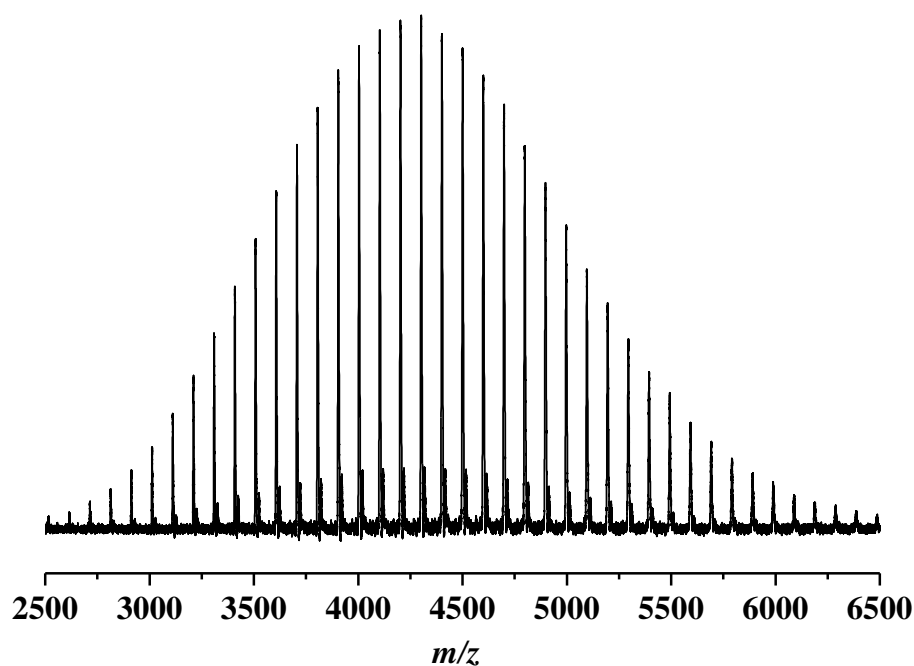


Figure S59: Full MALDI-ToF mass spectrum of **6d** with Na(CF₃COO) as cationization agent from a DCTB matrix in reflectron mode.

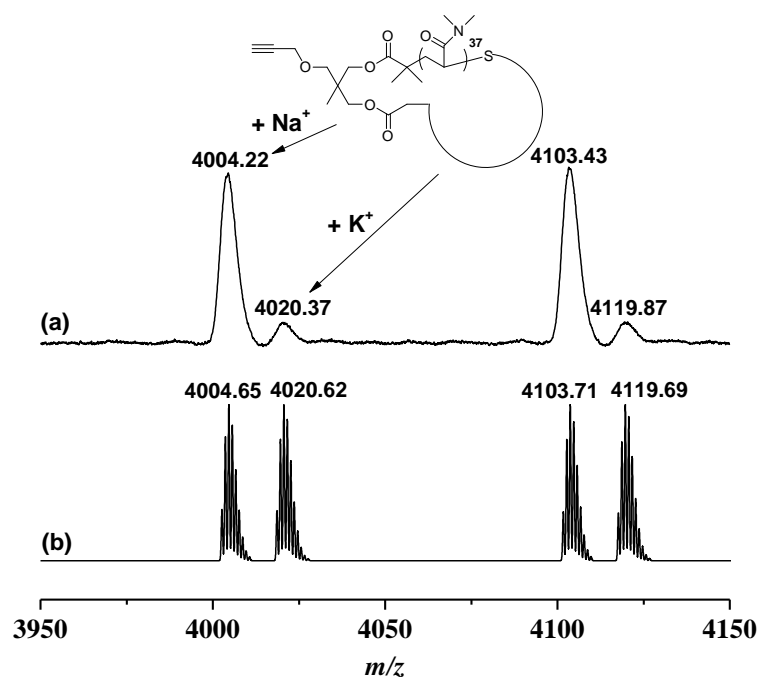


Figure S60: Expanded MALDI-ToF mass spectrum of **6d** with Na(CF₃COO) as cationization agent from a DCTB matrix in reflectron mode. (a) experimental isotopic resolution of peaks (b) theoretical isotopic pattern of products.

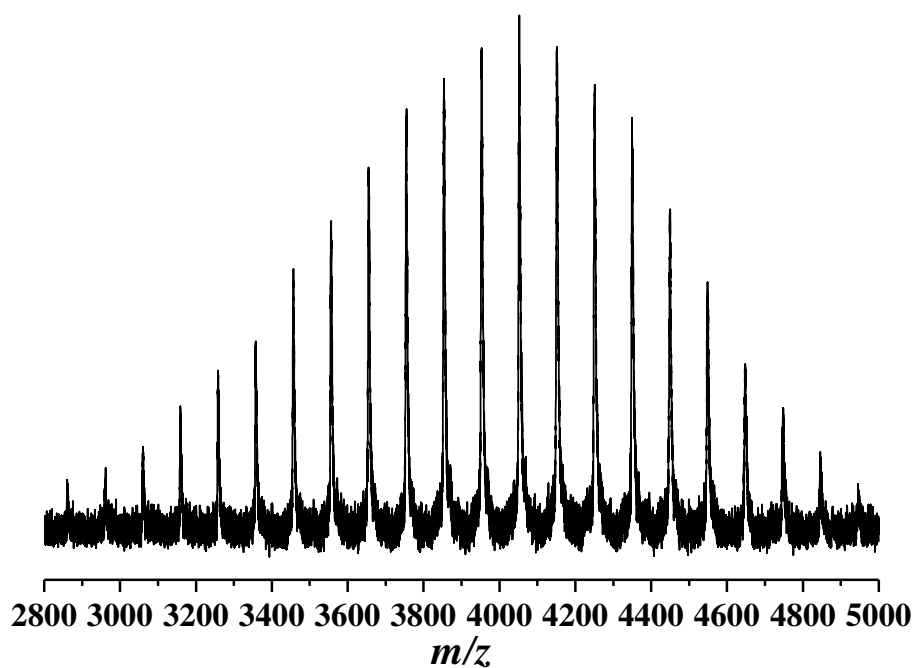


Figure S61: Full MALDI-ToF mass spectrum of **7d** with Na(CF₃COO) as cationization agent from a DCTB matrix in reflectron mode.

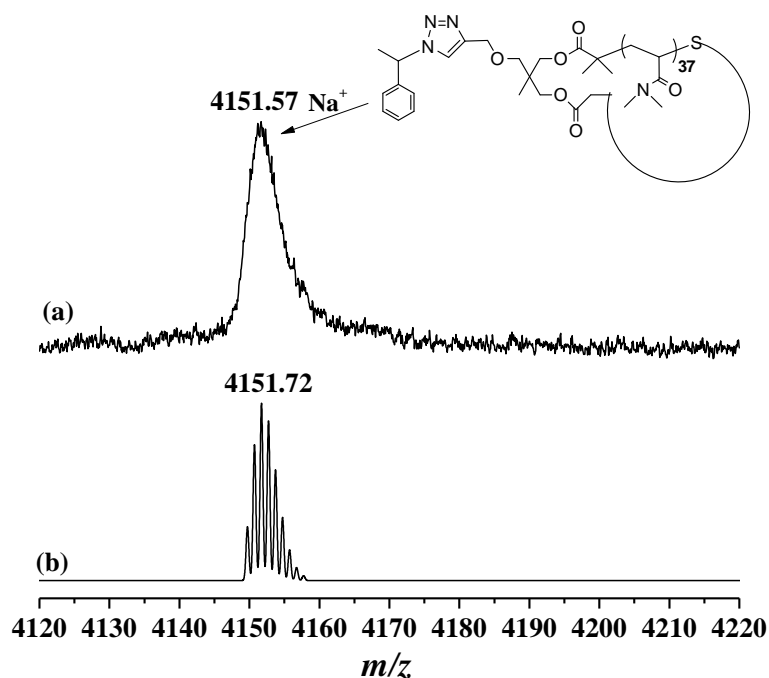


Figure S62: Expanded MALDI-ToF mass spectrum of **7d** with Na(CF₃COO) as cationization agent from a DCTB matrix in reflectron mode. (a) experimental isotopic resolution of peaks (b) theoretical isotopic pattern of products.

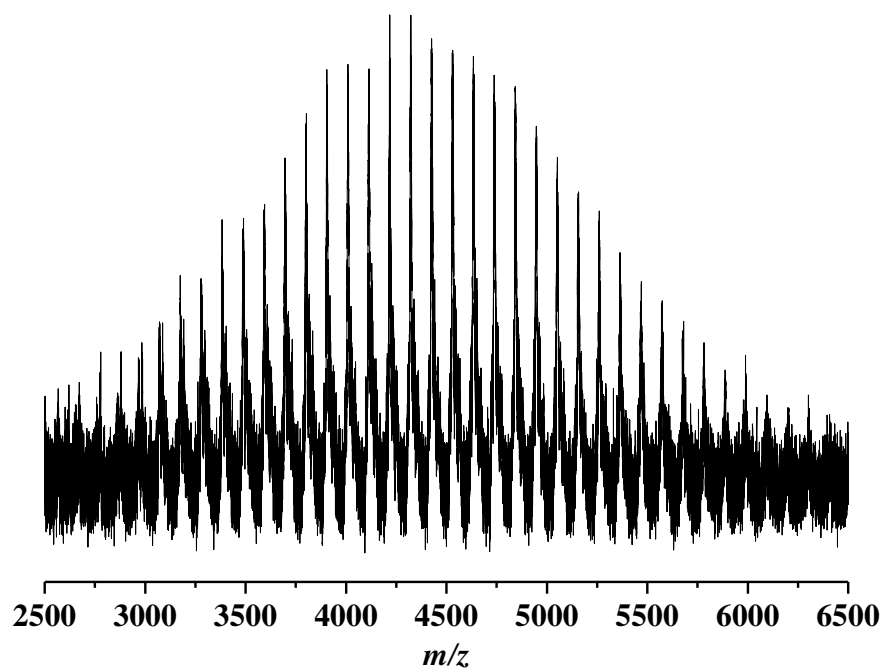


Figure S63: Full MALDI-ToF mass spectrum of **8** with $\text{Ag}(\text{CF}_3\text{COO})$ as cationization agent from a DCTB matrix in reflectron mode.

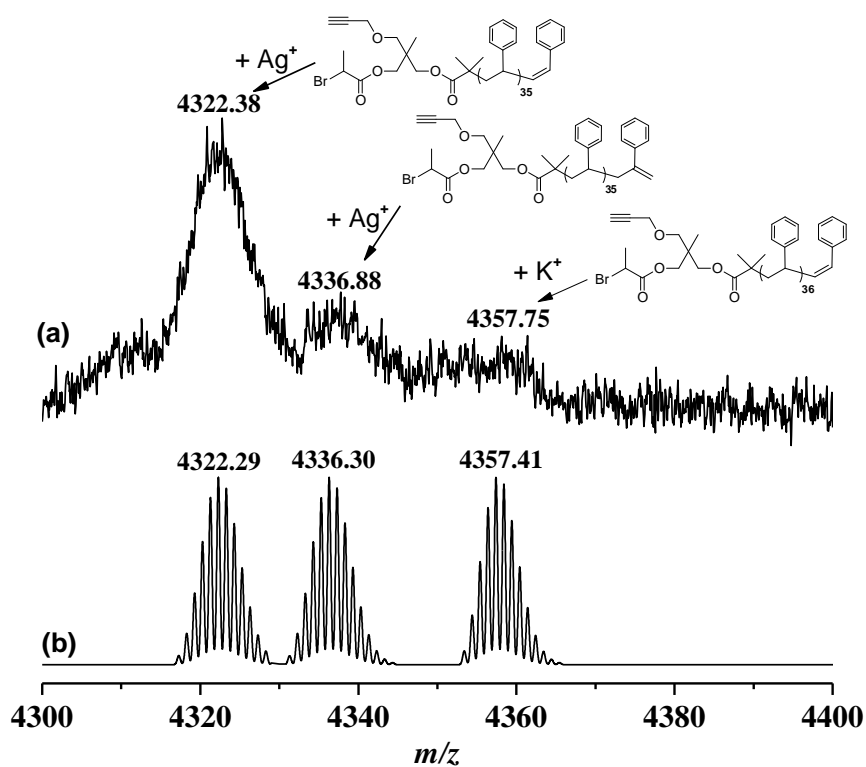


Figure S64: Expanded MALDI-ToF mass spectrum of **8** with $\text{Ag}(\text{CF}_3\text{COO})$ as cationization agent from a DCTB matrix in reflectron mode. (a) experimental isotopic resolution of peaks (b) theoretical isotopic pattern of products.

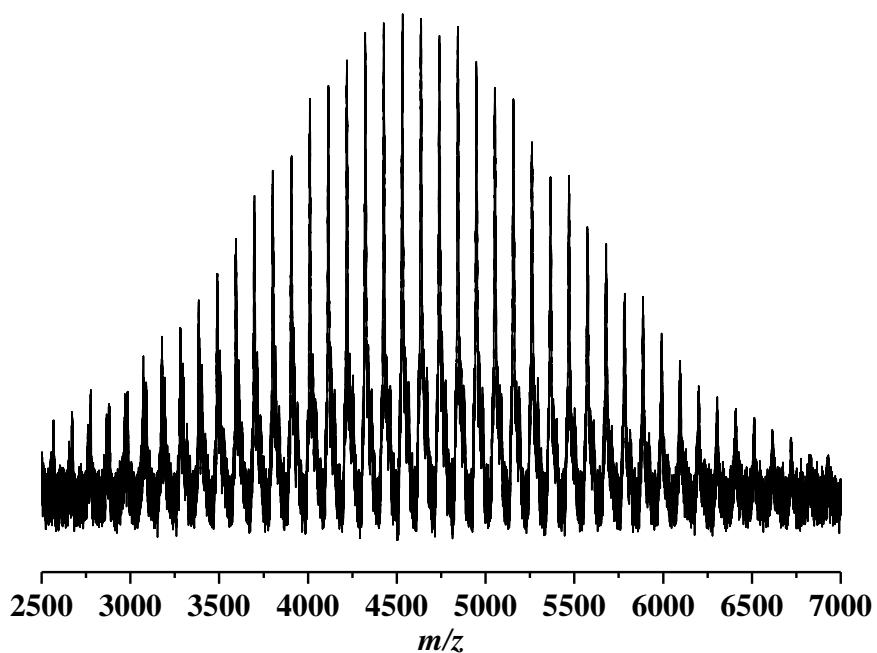


Figure S65: Full MALDI-ToF mass spectrum of **11** with $\text{Ag}(\text{CF}_3\text{COO})$ as cationization agent from a DCTB matrix in reflectron mode.

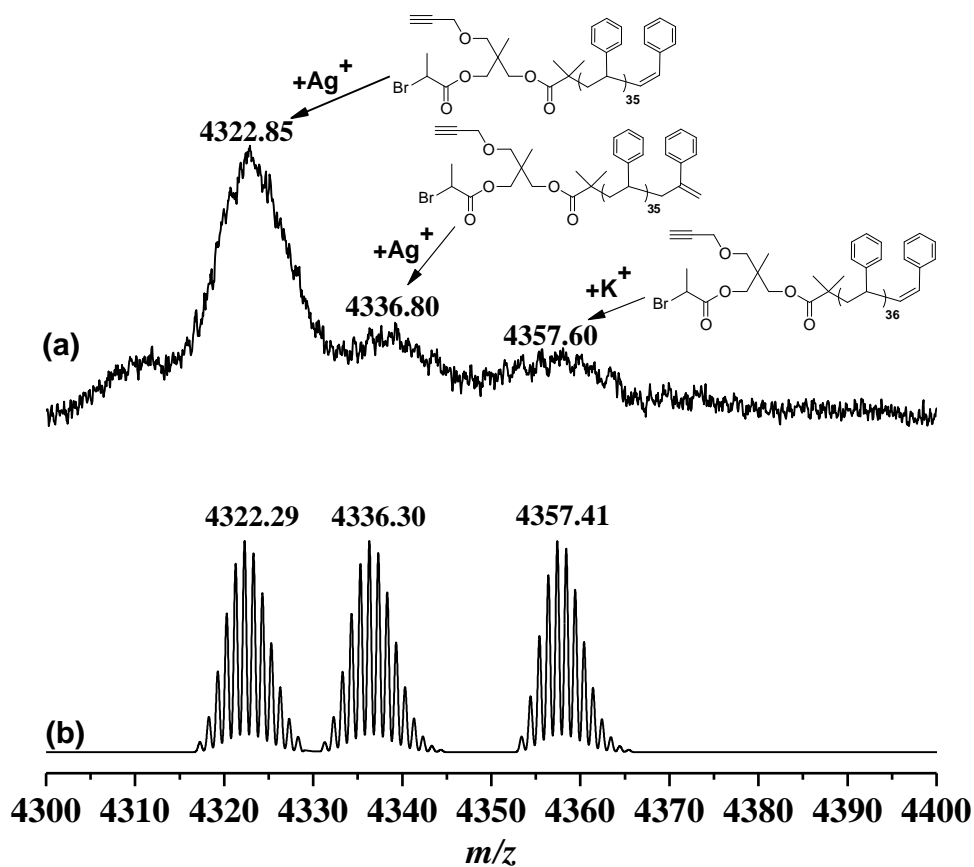


Figure S66: Expanded MALDI-ToF mass spectrum of **11** with $\text{Ag}(\text{CF}_3\text{COO})$ as cationization agent from a DCTB matrix in reflectron mode. (a) experimental isotopic resolution of peaks (b) theoretical isotopic pattern of products.

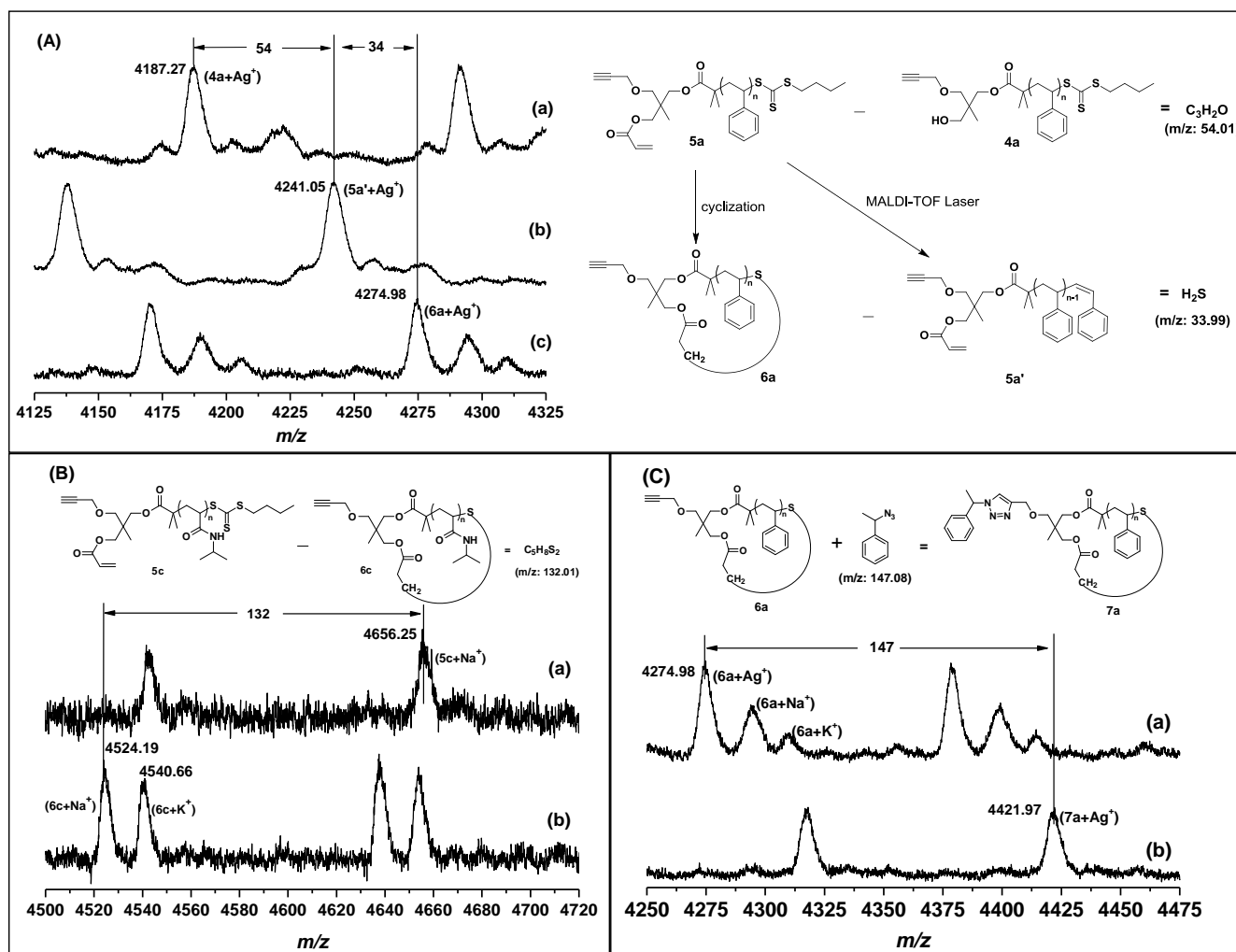


Figure S67: Expanded MALDI-TOF mass spectra comparison, for **4a**, **5a**, **6a** and **7a**, the spectra were acquired with $Ag(CF_3COO)$ as cationization agent, for **5c** and **6c** with $Na(CF_3COO)$ as cationization agent, and DCTB matrix in reflectron mode. (A) PSTY **4a** (a), PSTY **5a'** (b), and PSTY **6a** (c); (B) PNIPAm **5c** (a) and PNIPAm **6c** (b); and (C) PSTY **6a** (a) and PSTY **7a** (b). The schemes in the figure illustrated the formula change after the end-group modification and cyclization.

Reference:

- [1] Jia, Z. F.; Lonsdale, D. E.; Kulis, J.; Monteiro, M. J. *Acs Macro Lett* **2012**, *1*, 780-783.
- [2] Hossain, M. D.; Valade, D.; Jia, Z. F.; Monteiro, M. J. *Polymer Chemistry* **2012**, *3*, 2986-2995.